UNIVERSITY MICROFILMS, ANN ARBOR, MICH.

L. C. Card no. Mic 58-995

SMITH, Hadley James. A STUDY OF THE SWIRL VELOCITY AND THE STABILITY OF LAMINAR SWIRLING PIPE FLOW

University of Michigan, Ph. D., 1957
Engin. Mechanics

Negative microfilm received from university.

A STUDY OF THE SWIRL VELOCITY AND THE STABILITY OF LAMINAR SWIRLING PIPE FLOW

by
Hadley J. Smith

A dissertation submitted in partial fulfillment
of the requirements for the degree of
Doctor of Philosophy in the
University of Michigan
1956

Doctoral Committee

Professor John S. McNown, Chairman
Professor Glenn V. Edmonson
Professor Holger M. Hansen
Professor Arnold M. Kuethe
Professor Jesse Ormondroyd
Associate Professor Chia-Shun Yih

A STUDY OF THE SWIRL VELOCITY AND THE STABILITY OF LAMINAR SWIRLING PIPE FLOW

by Hadley J. Smith

The rotational component of velocity (swirl) and the stability of a steady, rotationally symmetric flow in a round pipe are studied analytically and experimentally. The flowing fluid is considered to be incompressible and viscous, and the assumptions of large Reynolds number in the laminar range and small swirl are used in linearizing the equations of motion.

If the upstream axial boundary condition on the swirl is arbitrary, solutions for the swirl include an expansion of orthogonal eigenfunctions which contain a form of the confluent hypergeometric function and which individually satisfy radial boundary conditions of the homogeneous Dirichlet type. The eigenfunction expansion has a suitable convergence for a broad range of axial boundary conditions, including an upstream radial distribution which is discontinuous at the wall of the pipe.

A particular case is considered in which an upstream boundary condition consisting of a prescribed swirl with a radial discontinuity is followed, respectively, by an axial region of growing swirl and one of decaying swirl. A solution for the swirl is compared with data obtained from tests

designed to approximate as closely as practicable the conditions assumed for the theory. At large radii, calculated values of the swirl rapidly approach the results of the experiments as the parameters approach the values assumed in linearizing. The solution is found to be useful at moderately large swirl. A new approximate solution, in which the swirl eigenfunctions are replaced by Bessel functions, is compared with the test data. It is found to be convenient for estimating the maximum swirl at various axial positions.

The problem of the hydrodynamic stability of laminar swirling pipe flow is formulated by the method of small oscillations as the first step in a preliminary investigation of the self-excitability of initially small, random disturbances. The resulting stability equation contains the laminar swirl solution as a coefficient. A study of the equation indicates that methods of solution, successful in analyzing the stability of Couette flow and some parallel flows, may be effective in the present case. Measured values of the conditions corresponding to the onset of visible instability indicate that self-excitation, if it occurs, takes place for parametric values bordering those for which the laminar swirl solution is most nearly accurate. The observed instability occurs in the region of axially decaying swirl.

ACKNOWLEDGMENTS

Appreciation is expressed to Professor J. S. McNown for his very helpful advice in orienting the author to the task of preparing a dissertation and for his patience and suggestions during the course of the work; to Professors H. M. Hansen and J. Ormondroyd for a number of helpful discussions; and to Professors G. V. Edmonson and W. W. Hagerty for information about practical problems related to the topic of this dissertation.

The author wishes to thank Professors R. C. F. Bartels, E. D. Rainville, and E. H. Rothe for suggesting mathematical references. Acknowledgment is made of a special indebtedness to Dr. P. Henrici and Mr. W. F. Cahill of the U. S. National Bureau of Standards for assistance in computations related to the swirl eigenfunctions which were performed on the Standards Eastern Automatic Computer. Appreciation is expressed to Mr. M. W. Kaufman for his friendly and invaluable assistance in the construction of the equipment and to Professor R. A. Dodge for his aid in securing funds and his kind cooperation throughout the course of the work.

The author expresses his endless thanks to his wife for her willing cooperation and never-failing optimism during the long period over which the work extended.

TABLE OF CONTENTS

		Page
ACKNOWLEDGEMENTS	. . . . .	ii
LIST OF TABLES	. . . . .	v
LIST OF ILLUSTRATIONS	. . . . .	vi
Chapter		
I.	INTRODUCTION	1
	1. The Scope of the Investigation	
	2. Relation to Earlier Studies	
	3. Related Engineering Problems	
II.	THE SWIRL VELOCITY DISTRIBUTION	8
	1. The Navier-Stokes and Continuity Equations	
	2. The Boundary Value Problem for the Swirl	
	3. Solution of the Swirl Boundary Value Problem	
III.	EVALUATION OF THE SWIRL EIGENFUNCTIONS AND RELATED QUANTITIES	22
	1. Computation of the Swirl Eigenfunctions	
	2. Solution for and Computation of the Normalizing Factors	
	3. Solution for and Computation of the Orthogonal Expansion Coefficients	
	4. Calculation of the Swirl Distribution	
IV.	APPROXIMATE SOLUTION FOR THE SWIRL	31
	1. Solution of the Swirl Equation by Successive Approximation Using Convergent Series	
	2. The Approximate Solution of the Swirl Boundary Value Problem	

Page

V. EXPERIMENTATION 38

1. Introductory Remarks
2. Experimental Apparatus
3. Incipient Instability
4. Measurement of the Swirl Velocity

VI. THE HYDRODYNAMIC STABILITY PROBLEM FOR LAMINAR SWIRLING FLOW 46

1. The Equations of Hydrodynamic Stability for Laminar Swirling Pipe Flow
2. Reduction of the Hydrodynamic Stability Equations to a Single Ordinary Differential Equation
3. Discussion of the Stability Problem

VII. CONCLUSIONS AND RECOMMENDATIONS 60

1. Concluding Remarks
2. Recommendations for Further Work

APPENDIX

I. THE PROPERTIES OF THE SWIRL EIGENVALUES AND EIGENFUNCTIONS 64

II. CONDITIONS FOR SMALL DEVIATION OF THE AXIAL VELOCITY FROM POISEUILLE DISTRIBUTION . 74

BIBLIOGRAPHY 81

LIST OF TABLES

Table		Page
1.	The Eigenvalues λ_n	23
2.	The Normalizing Factor $1/K_n^2$	26
3.	The Coefficients for the Orthogonal Expansion of $\bar{v}_o(r)$.	28
4.	Conditions for Which Swirl Was Computed.	29
5.	Comparison of the Exact and Approximate Eigenvalues	36
6.	Instability Appearing in the Decay Region of Laminar Swirling Flow	41

LIST OF ILLUSTRATIONS

Figure		Page
1.	Flow Boundaries, Co-ordinate System and Velocity Notation	86
2.	Values of the Parameters at the Inception of Instability in the Decay Region	87
3.	Eigenfunctions of the Exact and Approximate Swirl Solutions	88
4.	Radial Distribution of Swirl in the Decay Region	89
5.	Radial Distribution of Swirl in the Growth Region	90
6.	Radial Distribution of Swirl in the Decay Region	91
7.	Radial Distribution of Swirl in the Decay Region	92
8.	Axial Distribution of Swirl	93
9.	Radial Position of Maximum of Swirl in the Decay Region	94
10.	Axial Location of Incipient Instability vs. Reynolds Number of the Axial Flow	95
11.	Terms and Partial Sums of the Eigenfunction Expansion of $\bar{v}_o(r)$	96

CHAPTER I

INTRODUCTION

1. The Scope of the Investigation

The rotational component of velocity (swirl) and the stability of a steady, laminar, rotationally symmetric flow in a round pipe were studied analytically and experimentally. In the particular case considered, the flow passes through an axial region of swirl-growth and then through one of decay. The fluid is considered to be viscous and incompressible. The investigation was conducted to determine how nearly accurately the solutions of a linearized form of the Navier-Stokes equations describe the swirl and the stability of the flow as the conditions of linearization are approached.

In the theoretical portion of the work, a solution for the swirl was obtained and a preliminary analysis of the stability was performed. The experimentation consisted of measurements of the swirl and of the conditions corresponding to the onset of visible instability. The experiments were not intended to be exhaustive. Representative tests were performed and the results indicate that the theoretical approach is promising.

The swirl was generated by spinning a section of the pipe. The cylindrical co-ordinate system, velocity

notation, and boundaries for the flow are shown in Fig. 1. For theoretical purposes, it was assumed that the approach region was long enough for the establishment of Poiseuille flow. The length of the swirl-growth region was presumed to be arbitrary and that of the decay region to be infinite.

The resultant of the steady axial and swirl components will occasionally be referred to as the main flow in order to distinguish the latter from velocity perturbations such as disturbances.

2. Relation to Earlier Studies

In describing the relation of the present study to those of earlier investigators, it is helpful to consider the major phases of the problem which may be summarized as follows:

a. Preliminary steps

   Mathematical statement of the problem and linearization of the Navier-Stokes equations by consideration of orders of magnitude

b. Solution for the rate of decay of the swirl

   Partial solution of the steady swirl boundary value problem to determine the eigenvalues which correspond to the decay rates of individual harmonics of the swirl

c. Determination of the properties and values of the swirl eigenfunctions and related quantities

d. Completion of the swirl solution

   Expansion of the eigenfunctions expressing the radial dependence of the swirl harmonics to form a solution satisfying appropriate boundary and continuity conditions; derivation of a useful approximate solution

e. Formulation of the hydrodynamic stability problem

   Derivation of the equations governing the stability of swirling flow in light of earlier studies of plane flows, both straight and curved

f. Solution of the hydrodynamic stability problem to determine conditions for stability and instability

A flow of the type considered here was studied by Talbot [4][1] in 1951 and subsequently by others [1, 5] who largely duplicated or elaborated on the work of Talbot. Henrici [3] contributed more accurate values of the eigenvalues of the swirl eigenfunctions. Fortier [2] experimented with swirl in turbulent flow. The above works were concerned with the axial rate of decay of the swirl and did not obtain the swirl velocity. Consequently, previous work has been concerned primarily with items a and b of the above summary.

The order-of-magnitude argument of step a has not been explicitly presented heretofore. Possibly for this reason, some implications stemming from the linearization of the Navier-Stokes equations have not been fully appreciated and the potential usefulness of a velocity solution based on linear analysis may not have been foreseen. It is shown here that the assumptions implicit in the linearization rapidly become more realistic as the Reynolds number is increased and the swirl is decreased. The velocity solution

---

[1]Numbers in square brackets refer to entries in the Bibliography.

is found to be very nearly accurate when the Reynolds number is large or the swirl small. Because of the rapidity with which changes of these quantities are effective, the solution is useful even at moderately large swirl.

In earlier work, the axial rate of decay of the swirl, as predicted from the linearized analysis, appeared to correspond well with measurements. However, the comparison was indirect because only the decay rates of harmonics of the swirl were obtained from theory. Moreover, the initial conditions do not enter the analysis of decay and consequently the decay rates do not determine the swirl magnitude uniquely. Thus, a solution for the swirl velocity is needed to verify the results of previous studies.

After development of steps a and b of the above summary, the theoretical portion of the present paper carries the work through item e. The resulting linearized stability equations are more complex than those of previously solved stability problems. While the solution of these equations is a major task, it is likely that it will indicate the conditions for which swirling flow becomes unstable.

3. Related Engineering Problems

The present problem was selected primarily because it is fundamental in the field of mechanics. However, a description of one of the practical problems which may be be related to this study will facilitate later discussion.

Particular reference is made to the possible effect

of the transverse vibration of a pipeline on the friction loss in a normally laminar flow within the pipe. Such an effect in discharge lines has been reported by Vickers, Inc. Another case [6] has been encountered by personnel of the Trans-Arabian Oil Pipeline Company who have observed that desert winds above 20 miles per hour sometimes excite a complex vibration of a long suspended pipe line for which the Reynolds number of the flow was about 1000. The problem has been described and studied in several papers [6, 8, 10, 12] which, however, considered only the motion of the pipe and not the effect on the flow which was assumed to consist of ideal fluid with uniform velocity distribution. The results failed to indicate an explanation of the nature of the vibration in which the amplitude and frequency varied continuously between well defined limits. No consideration was given to the possibility of coupling between the motions of the pipe and of the viscous liquid flowing inside it.

From a review of the literature of pipe flow and hydrodynamic stability, it is conceivable that swirl instability is important in such cases. The line of thought is as follows. It is likely that a transverse vibration of a pipe, being normally of very small amplitude, could appreciably effect the friction losses in the flow only if it induced completely-developed turbulence or a periodically re-excited, turbulent-like condition [36, 44, 45]. It is well established experimentally that the laminar Poiseuille distribution of the axial velocity is very stable for Reynolds numbers

below approximately 2100. This stable velocity distribution would be essentially unaltered by a planar transverse vibration of the very small amplitudes encountered in practice because the fluid is incompressible.

However, a non-planar vibration of small amplitude may produce a swirl of appreciable magnitude in a long pipe. Such a secondary motion can assume profiles which are probably unstable, that is, which permit self-excitation of initially-small, random disturbances and lead to turbulent-like motion [4, 43]. These conditions would normally die out as the swirl decayed, if the Reynolds number were below 2100. However, if adjacent spans of the pipeline are vibrating 180° out of phase, as in the case of the Trans-Arabian pipeline, the fluid may pass alternately through regions of swirl growth and decay so that the disturbances are excited at intervals along the pipe axis. A substantial increase in friction loss would result and be accompanied by decrease in rate of flow. Because the momentum of the flow appears in the equations of motion for the pipe vibration, it is clear that there is a possibility of significant coupling which can be explained only if the viscosity of the fluid is taken into account. One growth and one decay region are represented in the problem of this dessertation.

The hypothetical instability of the swirl is not the only plausible method by which the transverse vibration of the pipe may induce turbulence. For instance, to some extent a growing or decaying swirl actually distorts the

axial velocity from the Poiseuille distribution so that it, as well as the swirl profile, may be unstable [18]. Or, if the vibration amplitude is appreciable, the moving, curved path of the flow can result in unstable distributions of the axial flow. In some instances, instability may be at most a secondary cause and the disturbances leading to turbulence may be a steady state, resonant response of the fluid to an oscillating pressure gradient or other forcing condition having its origin in the vibration of the pipe.[2] It is possible that a number of fundamental studies may be required to understand the mechanics of the vibrating pipeline.

---

[2]See [29] for an example of a similar phenomenon in a boundary layer.

CHAPTER II

THE SWIRL VELOCITY DISTRIBUTION

1. The Navier-Stokes Equations and The Continuity Equation

The dimensionless Navier-Stokes equations for the rotationally symmetric motion of an incompressible fluid are, in the notation of Fig. 1,

$$(1)\qquad \frac{\partial u}{\partial t}+u\frac{\partial u}{\partial r}+w\frac{\partial u}{\partial z}-\frac{v^2}{r}=-\frac{\partial p}{\partial r}+\frac{1}{R}\left(\nabla_1^2 u-\frac{u}{r^2}\right)$$

$$(2)\qquad \frac{\partial v}{\partial t}+u\frac{\partial v}{\partial r}+w\frac{\partial v}{\partial z}+\frac{uv}{r}=\frac{1}{R}\left(\nabla_1^2 v-\frac{v}{r^2}\right)$$

$$(3)\qquad \frac{\partial w}{\partial t}+u\frac{\partial w}{\partial r}+w\frac{\partial w}{\partial z}=-\frac{\partial p}{\partial z}+\frac{1}{R}\nabla_1^2 w$$

and the continuity equation is

$$(4)\qquad \frac{1}{r}\frac{\partial (ru)}{\partial r}+\frac{\partial w}{\partial z}=0$$

In the above equations ∇_1^2 is the two-dimensional Laplacian operator

$$(5)\qquad \nabla_1^2=\frac{\partial^2}{\partial r^2}+\frac{1}{r}\frac{\partial}{\partial r}+\frac{\partial^2}{\partial z^2}$$

and R is the Reynolds number of the axial flow and is given by

$$(6)\qquad R=\frac{\bar{w}_m a}{\nu}$$

where a is a characteristic length taken as the radius of the

pipe, ν is the kinematic viscosity of the fluid, and $\bar{w}_m$ (the peak velocity in Poiseuille flow) is defined as

(7) $$w_m = \frac{2Q}{A}$$

in which Q is the volumetric rate of flow and A is the area of the pipe cross-section. If a bar indicates the original (dimensional) quantities, the independent and dependent variables in equations (1) through (4) have been made dimensionless as follows:

(8) $$r = \frac{\bar{r}}{a} \qquad z = \frac{\bar{z}}{a} \qquad t = \frac{\bar{t}}{(a/\bar{w}_m)}$$

(9) $$u = \frac{\bar{u}}{\bar{w}_m} \qquad v = \frac{\bar{v}}{\bar{w}_m} \qquad w = \frac{\bar{w}}{\bar{w}_m} \qquad p = \frac{\bar{p}}{\rho \bar{w}_m^2}$$

Coriolis and gravitational terms representing body forces have been omitted from (1) through (3). The former were assumed to be negligible. The latter were eliminated by defining p as the dimensionless total pressure less a portion corresponding to the ordinary hydrostatic pressure which would exist if the fluid were static.

If p is eliminated from equations (1) and (3) by cross-differentiation and subtraction, equations (1), (3), and (4) can be reduced to

(10) $$\left[D_t - \frac{u}{r} - \frac{1}{\mathcal{R}} \textcircled{H} \right] \textcircled{H} \psi = -\frac{\partial}{\partial z}\left(\frac{v^2}{r}\right)$$

and equation (2) can be written directly as

(11) $$\left[D_t + \frac{u}{r} - \frac{1}{\mathcal{R}} \textcircled{H} \right] v = 0$$

where

$$D_t \equiv \frac{\partial}{\partial t} + u\frac{\partial}{\partial r} + w\frac{\partial}{\partial z} \tag{12}$$

$$\textcircled{H} \equiv \frac{\partial^2}{\partial r^2} + \frac{1}{r}\frac{\partial}{\partial r} - \frac{1}{r^2} + \frac{\partial^2}{\partial z^2} = \nabla_1^2 - \frac{1}{r^2} \tag{13}$$

and the stream function ψ is defined by

$$u = -\frac{1}{r}\frac{\partial(r\psi)}{\partial z} = -\frac{\partial \psi}{\partial z} \tag{14}$$

$$w = \frac{1}{r}\frac{\partial(r\psi)}{\partial r} = \frac{\partial \psi}{\partial r} + \frac{\psi}{r} \tag{15}$$

which satisfy the continuity equation (4). The system (1) through (4) can thus be reduced to the system (10) and (11).

It will be convenient to define the operator

$$L \equiv \frac{\partial^2}{\partial r^2} + \frac{1}{r}\frac{\partial}{\partial r} - \frac{1}{r^2} = \textcircled{H} - \frac{\partial^2}{\partial z^2} \tag{16}$$

Thus

$$L(\psi) = \frac{\partial}{\partial r}\left[\frac{1}{r}\frac{\partial(r\psi)}{\partial r}\right] = \frac{\partial w}{\partial r} \tag{17}$$

and

$$\textcircled{H}\psi = L(\psi) + \frac{\partial^2 \psi}{\partial z^2} = \frac{\partial w}{\partial r} - \frac{\partial u}{\partial z} = \zeta_\theta \tag{18}$$

where ζ_θ is the vorticity in the r-z plane.

2. The Boundary Value Problem for the Swirl

The distribution of the swirl is required for the

range of conditions in which it is laminar and especially for that part of the range bordering the onset of instability. In the following analysis of the flow, an occasional mention of certain test results has been included so as to provide perspective on the underlying limitations and approximations. The experimentation will be described in detail in Chapter V.

The swirl parameter $\mathcal{S}$ is defined as

(19) $$\mathcal{S} = \frac{\Omega a}{\bar{w}_m}$$

For the equipment used in the present work, incipient instability appeared in the decay region for a value of $\mathcal{R}$ which depended on $\mathcal{S}$, as shown in Fig. 2. Therefore, the solution for laminar swirling flow will be valid only for values of $\mathcal{R}$ and $\mathcal{S}$ for which the flow is stable.

The orders of magnitude of w and of the operator $\frac{\partial}{\partial r}$ are defined to be unity, that is,

(20) $$w = O(1) \qquad \frac{\partial}{\partial r} = O(1)$$

The boundary-layer-type assumption, $\frac{\partial}{\partial z} < \frac{\partial}{\partial r}$, is made. Thus,

(21) $$\frac{\partial}{\partial z} = O(-1)$$

As indicated by the measurements plotted in Fig. 8, this approximation is plausible for the swirl if r and z^* or z are large. If z^* or z is small, (21) may still be reasonable at radii close to the wall where, intuitively, $\frac{\partial v}{\partial r}$ is very large in absolute value.

Velocity components w_1 and w_2 are defined as follows:

(22) $$w(r, z) = w_1(r) + w_2(r, z) = (1 - r^2) + w_2(r, z)$$

(23) $$w_1 = O(1) \qquad w_2 = O(-2)$$

where w_1 is the Poiseuille distribution of axial flow. Then, by (4) and (23), we have

$$|u(r,z)| = \left|-\frac{1}{r}\int_0^r \frac{\partial w_2(x,z)}{\partial z}\, x\, dx\right| \le \frac{1}{r}\int_0^r \left|\frac{\partial w_2(r,z)}{\partial z}\right| x\, dx$$

$$\le \frac{r}{2}\left|\frac{\partial w_2(r,z)}{\partial z}\right|_{max} \equiv O\left(\frac{\partial w_2}{\partial z}\right)$$

This result depends only on the boundary layer approximation and continuity and, from (21) and (23),

(24) $$u = O(-3)$$

For a steady flow, equations (11) and (22) may be combined to obtain

(25) $$u\frac{\partial v}{\partial r} + (1-r^2)\frac{\partial v}{\partial z} + w_2\frac{\partial v}{\partial z} + \frac{uv}{r} = \frac{1}{R}\left(\frac{\partial^2 v}{\partial r^2} + \frac{1}{r}\frac{\partial v}{\partial r} - \frac{v}{r^2} + \frac{\partial^2 v}{\partial z^2}\right)$$

Assuming that a useful solution may be obtained by dropping from (25) the terms which have been assumed to be of small order, and utilizing (20) through (24), the orders of magnitude of the terms in (25) are, respectively,

(26) $$O(-3)\cdot O(v) + O(1)\cdot O(v) + O(-2)\cdot O(v) + O(-3)\cdot O(v)$$

$$= \frac{1}{R}\left[O(1) + O(1) - O(1) + O(-2)\right] O(v)$$

If the terms of lowest order in (25) are dropped, there results the linear, homogeneous, partial differential equation in v

$$(1-r^2)\frac{\partial v}{\partial z} = \frac{1}{R}\left(\frac{\partial^2 v}{\partial r^2} + \frac{1}{r}\frac{\partial v}{\partial r} - \frac{v}{r^2}\right)$$

or

$$\frac{\partial v^2}{\partial r^2} + \frac{1}{r}\frac{\partial v}{\partial r} + \left[-R(1-r^2)\frac{\partial}{\partial z} - \frac{1}{r^2}\right]v = 0 \qquad \begin{matrix}(0<r<1)\\(0<z)\\(0<z^*<\ell)\end{matrix} \tag{27}$$

which will be referred to as the swirl equation. This result was given in [4] but without exhibiting the order-of-magnitude argument which is of great value in assessing the usefulness of the solution for the swirl. Except for occasional points identified by references, we now depart from earlier work.

We stipulate the following boundary conditions on $v(r,z)$ in the decay region of Fig. 1

$$v(0,z) = 0 \qquad (0<z) \tag{28}$$

$$v(1,z) = 0 \qquad (0<z) \tag{29}$$

$$v(r,0) = v_0(r) \qquad (0<r<1) \tag{30}$$

$$v(r,\infty) = 0 \qquad (0<r<1) \tag{31}$$

and the boundary conditions on $v(r,z^*)$ in the growth region of Fig. 1 are taken as

(32) $$v(0, \tau^*) = 0 \qquad (0 < \tau^* < \ell)$$

(33) $$v(1, \tau^*) = \delta \qquad (0 < \tau^* < \ell)$$

(34) $$v(r, \tau^*)_{\tau^*=0} = v_0^*(r) \qquad (0 < r < 1)$$

(35) $$v(r, \tau^*)_{\tau^*=\ell} = v_\ell^*(r) \qquad (0 < r < 1)$$

In the foregoing and all later boundary conditions, terms such as $v(0, \tau)$ and $v(1, \tau)$ are defined as

$$v(0, \tau) = \lim_{r \to 0(+)} v(r, \tau) \qquad v(1, \tau) = \lim_{r \to 1(-)} v(r, \tau)$$

in order to avoid unnecessarily restrictive boundary conditions. The function $v_0^*(r)$ is defined as

(36) $$v_0^*(r) = 0 \qquad (0 \leq r < 1)$$
$$= \delta \qquad (r = 1)$$

The functions $v_\ell^*(r)$ and $v_0(r)$ will be determined by continuity considerations.

3. Solution of the Swirl Boundary Value Problem

If substitution of the separated form of solution

$$v(r, \tau) = R(r) e^{-\beta \tau}$$

where β is a constant, and the relation

$$\mathcal{R} \beta = 16 \lambda^2$$

in (27) results in a solution, the latter will be unique because (27) is parabolic and conditions (28), (29), (31), and (32) are of the homogeneous Dirichlet type [54, p. 706].

Thus

$$\frac{d^2R}{dr^2} + \frac{1}{r}\frac{dR}{dr} + \left[16\lambda^2(1-r^2) - \frac{1}{r^2}\right]R = 0 \tag{37}$$

The singularities of this equation are limited to a regular singular point at $r=0$, an irregular singular point at $r=\infty$ and a singularity at $\lambda=\infty$ which we shall not classify. Consequently, all solutions will be analytic functions of r and λ at least for all finite values of r and λ except, at most, at $r=0$. Thus those solutions which also satisfy the homogeneous Dirichlet conditions, (28) and (32), will be analytic for all finite r and λ, at least. The fundamental system of solutions of (37) is given partially in [4] and partially in [46] and leads to the following linearly independent solutions of (27).

$$v_{(1)} = R(r)e^{-\beta z} = \left[2\lambda^{1/2} r\, e^{-2\lambda r^2}\, \phi(1-\lambda, 2; 4\lambda r^2)\right] e^{-\beta z} \tag{38}$$

$$v_{(2)} = R_{(2)}(r)e^{-\beta z} = \left[\ln(4\lambda r^2)R(r) + \sum_{j}^{\infty} A_j(\lambda, z)\frac{(4\lambda r^2)^j}{j!}\right]e^{-\beta z} \tag{39}$$

Here ϕ is Humbert's symbol for the confluent hypergeometric function so that [49]

$$\phi(a, c; x) \equiv {}_1F_1(a, c; x)$$

which, if neither a nor c is a negative integer, is given by Kummer's series

$$\phi(a, c; x) = 1 + \frac{a}{c}\frac{x}{1!} + \frac{a(a+1)}{c(c+1)}\frac{x^2}{2!} + \cdots = \sum_{1}^{\infty}\frac{(a)_m}{(c)_m}\frac{x^m}{m!} \tag{40}$$

which is readily shown to be uniformly and absolutely convergent. For convenience, terms of the form (38) will be referred to as swirl harmonics even though they are not harmonic functions.

If a solution of the form

$$v = v(r)$$

is assumed, (27) reduces to the Cauchy equation which has the fundamental set of solutions

$$v_{(3)} = r \qquad v_{(4)} = \frac{1}{r} \tag{41}$$

A solution of the form $v = v(z)$ cannot satisfy (27).

In the decay region, boundary conditions (28) and (29) can be met only by $v_{(1)}$ and, in view of the linearity of (27), the solution for the swirl is

$$v = \sum_{1}^{N} d_n R_n(r) e^{-\beta_n z} \qquad (0 < z) \tag{42}$$

where the d_n are constants and N is any positive integer. This solution satisfies (28) by inspection and (29) is satisfied if λ assumes the discrete eigenvalues λ_n for which

$$\phi(1-\lambda_n, 2; 4\lambda_n r^2)_{r=1} = 0 \qquad (n = 1, 2, \cdots) \tag{43}$$

in which the positive integers n have a one-to-one correspondence with the λ_n arranged in ascending order. The existence of the values λ_n is shown Appendix I.

Condition (31) is satisfied because the numbers

$$\beta_m = \frac{16\lambda_m^2}{R}$$

are positive, as shown in Appendix I. The remaining condition for the decay region, (30), will be considered shortly.

In the growth region, the conditions (32) through (35) apply. It is readily seen that a solution which satisfies (32) and (33) is

(44) $$v = Ar - \sum_1^N b_m R_m(r) e^{-\beta_m z^*} \qquad (0 < z^* < l)$$

This solution also satisfies

(32) $$v(r, z^*)_{z^*=0} = v_0^*(r)$$

where

(36) $$v_0^*(r) = 0 \qquad (0 \le r < 1)$$
$$= A \qquad (r = 1)$$

if

(45) $$\sum_1^N b_m R_m(r) \simeq \bar{v}_0(r)$$

where

(46) $$\bar{v}_0(r) = Ar \qquad (0 \le r < 1)$$
$$= 0 \qquad (r = 1)$$

In Appendix I, it is proved that the series (45) is an orthogonal expansion in $R_n(r)$ which, at least if N is finite and a minimum of three, closely approximates $\bar{v}_o(r)$. The proof in Appendix I is necessary because the eigenfunctions R_n are generated by the system (37), (28), and (29) which is a singular case of the Sturm-Liouville boundary value problem. Thus the common method of proving the convergence of eigenfunction expansions, that of citing the Sturm-Liouville theory, cannot be used to verify (45). Other results obtained in Appendix I are

$$b_m = \frac{1}{K_m^2} \int_0^1 r(1-r^2)\, \bar{v}_o(r) R_m(r)\, dr \qquad (m \le N) \tag{47}$$

where $\frac{1}{K_m^2}$ is the normalizing factor and

$$K_m^2 = \int_0^1 r(1-r^2) R_m^2(r)\, dr \tag{48}$$

R_n/K_n are the normalized eigenfunctions, orthogonal in $0 \le r \le 1$ with respect to the weight function $r(1-r^2)$, That is,

$$\int_0^1 r(1-r^2)\left(\frac{R_i}{K_i}\right)\left(\frac{R_j}{K_j}\right) = \delta_{ij} \tag{49}$$

There remains the task of satisfying equations (30) and (35) which require continuity of the swirl at $z = 0$ for all r, except $r = 1$ where the boundary conditions are discontinuous. Equating (42) and (44) for $z = 0$ and $z^* = \ell$, respectively,

(50) $$\sum_1^N d_m R_m(r) = \mathcal{S}r - \sum_1^N b_m R_m(r) e^{-\beta_m l}$$
$$\cong \sum_1^N b_m R_m(r) - \sum_1^N b_m R_m(r) e^{-\beta_m l} \qquad (0 \le r < 1)$$

and

$$\sum_1^N d_m R_m(r) = \sum_1^N (1 - e^{-\beta_m l}) b_m R_m(r)$$

whence,

$$d_m = (1 - e^{-\beta_m l}) b_m$$

and in the decay region

(51) $$v \cong \sum_1^N (1 - e^{-\beta_m l}) b_m R_m(r) e^{-\beta_m z} \qquad (0 < z)$$

It is now convenient to examine the significance of the assumption that

(23) $$w_z = O(-z)$$

In Appendix II it is shown that when the boundary layer approximation is valid, a necessary condition for (23) is that the swirl be of small magnitude, that is,

(52) $$v = O(1)$$

In the present problem, a necessary condition consists of (52) or, alternately, is that

a. $\mathcal{R}$ be increased sufficiently,

b. $\mathcal{A}$ be decreased sufficiently, or

c. ℓ be decreased sufficiently

This development (52) does not change the results of the order-of-magnitude argument employed in obtaining the swirl equation (27), since in that process no assumption was made as to the order of the swirl. Referring to Fig. 2, it is seen that, at incipient instability, the swirl solution may be most accurate at the higher values of $\mathcal{R}$ where the corresponding values of $\mathcal{A}$ are small.

Collecting the results of this section, we have the following solution of the linearized swirl problem, (27) through (35)

$$v \cong \mathcal{A} r - \sum_{1}^{N} b_m R_m(r) e^{-\beta_m z^*} \qquad (0 < z^* < \ell) \tag{44}$$

$$v \cong \sum_{1}^{N} (1 - e^{-\beta_m \ell}) b_m R_m(r) e^{-\beta_m z} \qquad (0 < z) \tag{51}$$

which may be a realistic description of the flow if

a. the order of the swirl be relatively small, that is,

$$v = O(-1) \tag{52}$$

b. the solution of the Navier-Stokes equations, linearized for small swirl, be asymtotic to the solution of the exact, non-linear Navier-Stokes equations as the swirl decreases.

The investigation of the second contingency was the primary purpose of the measurements of the swirl which will be described in Chapter V.

CHAPTER III

EVALUATION OF THE SWIRL FUNCTIONS AND RELATED QUANTITIES

1. Computation of the Swirl Functions

The swirl eigenfunctions, R_n, are given by

$$R_n(r) = 2\lambda_n^{3/2} r e^{-2\lambda_n r^2} \phi(1-\lambda_n, 2; 4\lambda_n r^2) \tag{53}$$

The confluent hypergeometric function, $\phi(1-\lambda_n, 2; 4\lambda_n r^2)$ and the function

$$\phi(2-\lambda_n, 3; 4\lambda_n r^2) = \frac{2}{1-\lambda_n} \phi'(1-\lambda_n, 2; 4\lambda_n r^2) \tag{54}$$

where

$$\phi'(1-\lambda_n, 2; x) \equiv \frac{d\phi}{dx} \tag{55}$$

were calculated to ten significant figures based on equation (40) and utilizing the National Bureau of Standards Eastern Automatic Computer (SEAC). The work was done at the request of the author by personnel of the Bureau, and was carried out for the first three eigenvalues (λ_1, λ_2, and λ_3). The author then used (53) to compute the first three eigenfunctions (R_1, R_2, and R_3). The results are plotted in

Fig. 3.

In this work, use was made of eigenvalues which were also computed on SEAC utilizing equations (40) and (43). These values are given to seven figures in Table 1 and are due to Henrici [3].

TABLE 1

THE EIGENVALUES λ_n

n	λ_n
1	1.156025
2	2.161876
3	3.163755
4	4.164640
5	5.165143

Higher values of λ_m can be readily computed from the asymptotic expressions given in [3] and [51]. In applications, values of λ_m beyond λ_5 are seldom necessary, and in the present problem good results were obtained using only λ_1, λ_2, and λ_3.

2. Solution for and Computation of the Normalizing Factors

In order to determine the value of the normalizing factor, $1/K_n^2$, it is necessary to evaluate the integral

$$K_n^2 = \int_0^1 r(1-r^2) R_m^2(r)\, dr \tag{48}$$

This integral was evaluated and computed in the course of the present work. Only a summary of the method is required.

The functions $R(\lambda, 2, r)$ are solutions of the swirl equation

$$\frac{d^2R}{dr^2} + \frac{1}{r}\frac{dR}{dr} + \left[16\lambda^2(1-r^2) - \frac{1}{r^2}\right]R = 0 \tag{37}$$

The special Whittaker function, $M_{\lambda,\frac{1}{2}}(a_2 y)$, where λ and a_2 are constants, is a solution [48] of

$$\frac{d^2M}{dy^2} + \left[-\frac{a_2^2}{4} + \frac{a_2^2\lambda}{y}\right]M = 0 \tag{57}$$

and since [48, p. 12]

$$M_{\lambda,\frac{1}{2}}(a_2 y) = (a_2 y)^{\frac{1}{2}} R(\lambda, 2, a_2 y) \tag{58}$$

we obtain

$$M_{\lambda,\frac{1}{2}}(4\lambda r^2) = 2\lambda^{1/2} r\, R(\lambda, 2, 4\lambda r^2) \tag{59}$$

so that conclusions reached with respect to $M_{\lambda,\frac{1}{2}}(a_2 y)$ can be transformed into conclusions about $R(\lambda, 2, r) \equiv R(r)$.

Let $M_{\chi,\frac{1}{2}}(a_1 y)$ be a second function which satisfies

$$\frac{d^2M}{dy^2} + \left[-\frac{a_1^2}{4} + \frac{a_1\chi}{y}\right]M = 0 \tag{60}$$

Multiplying (57) by $M_{\chi,\frac{1}{2}}$ and (60) by $M_{\lambda,\frac{1}{2}}$ and subtracting, the following integral equation may be written

$$\int_0^y \left\{\frac{a_2^2 - a_1^2}{4} + \frac{\chi a_1 - \lambda a_2}{\xi}\right\} M_{\chi,\frac{1}{2}}(a_1\xi) M_{\lambda,\frac{1}{2}}(a_2\xi)\, d\xi$$

$$= -\int_0^y \left\{M_{\lambda,\frac{1}{2}} \frac{d^2M_{\chi,\frac{1}{2}}}{d\xi^2} - M_{\chi,\frac{1}{2}} \frac{d^2M_{\lambda,\frac{1}{2}}}{d\xi^2}\right\} d\xi$$

$$= \int_0^y d\left\{ M_{\chi,\frac{1}{2}}(a_1,\xi)\frac{d}{d\xi}M_{\lambda,\frac{1}{2}}(a_2,\xi) - M_{\lambda,\frac{1}{2}}(a_2,\xi)\frac{d}{d\xi}M_{\lambda,\frac{1}{2}}(a_1,\xi)\right\}$$

$$= \begin{vmatrix} M_{\chi,\frac{1}{2}}(a_1,y) & M_{\lambda,\frac{1}{2}}(a_2,y) \\ \frac{d}{dy}M_{\chi,\frac{1}{2}}(a_1,y) & \frac{d}{dy}M_{\lambda,\frac{1}{2}}(a_2,y) \end{vmatrix}$$

Letting $a_1 = 4\chi$ and $a_2 = 4\lambda$, dividing by $(\lambda - \chi)$, letting $\lambda = \lambda_m$, taking the limit as $\chi \to \lambda_n$, letting $y = r^2$, and utilizing (59), there results

$$(61) \qquad K_n^2 = \int_0^1 r(1-r^2)R_n^2\,dr = \lambda_n e^{-4\lambda_n}\phi_n'(4\lambda_n r^2)\Big|_{r=1} \cdot \frac{\partial}{\partial\lambda}\phi(4\lambda)\Big|_{\lambda=\lambda_n}$$

Because ϕ is uniformly convergent, we may differentiate it termwise and, after some additional manipulation,

$$(62) \qquad \frac{\partial}{\partial\lambda}\phi(4\lambda)\Big|_{\lambda=\lambda_n} = 2(1-\lambda_n)\phi(2-\lambda_n,3;4\lambda_n) - \sum_{m=0}^{\infty}\left[\psi(1-\lambda_n+m)-\psi(1-\lambda_n)\right]\frac{(1-\lambda_n)_m(4\lambda_n)^m}{(2)_m\,m!}$$

where $\psi(a) \equiv \frac{d}{da}\left[\ln\Gamma(a)\right]$. Then from (61), (62), and (54)

$$(63) \qquad K_n^2 = \frac{\lambda_n(1-\lambda_n)}{2}e^{-4\lambda_n}\phi(2-\lambda_n,3;4\lambda_n)\cdot \left\{2(1-\lambda_n)\phi(2-\lambda_n,3;4\lambda_n) - f(\lambda_n)\right\}$$

where f(λ_n) indicates the series in (62). The values of $\frac{1}{K_n^2}$ were calculated manually by the author from (63) using a self-checking procedure. It was necessary to sum about twenty-five terms of each of the several series involved in order to obtain the values of the normalizing factor, $\frac{1}{K_m^2}$, to four significant figures as given in Table 2.

TABLE 2

THE NORMALIZING FACTOR $1/K_n^2$

n	$1/K_n^2$
1	21.62
2	74.96
3	160.3

3. Solution for and Computation of the Orthogonal Expansion Coefficients

The coefficients of the orthogonal expansion (45) are

(47) $$b_n = \frac{1}{K_n^2} \int_0^1 r(1-r^2)\, \bar{v}_0(r)\, R_n(r)\, dr \qquad (n \le N)$$

where

(46) $$\bar{v}_0(r) = \mathcal{L} r \qquad (0 \le r < 1)$$
$$= 0 \qquad (r = 1)$$

The swirl functions R_n satisfy

(64) $$\begin{cases} \dfrac{d^2 R_n}{dr^2} + \dfrac{1}{r}\dfrac{dR_n}{dr} + \left[16\lambda_n^2(1-r^2) - \dfrac{1}{r^2}\right] R_n = 0 \\ R_n(0) = R_n(1) = 0 \end{cases}$$

The differential equation in (64) may be written

$$\frac{d}{dr}\left[\frac{1}{r}\frac{d}{dr}(rR_n)\right] + 16\lambda_n^2(1-r^2)R_n = 0 \tag{65}$$

Substituting (46) and (65) in (47), and using (64),

$$16\lambda_n^2 K_n^2 \frac{b_n}{\ell} = -\int_0^1 r^2\, d\left[\frac{1}{r}\frac{d}{dr}(rR_n)\right] \tag{66}$$

$$= -\left\{\left[rR_n + r^2\frac{dR_n}{dr}\right]_0^1 - 2\int_0^1 d(rR_n)\right\}$$

$$= -\left\{\frac{d}{dr}(R_n)_{r=1} - 2\left[rR_n\right]_0^1\right\}$$

$$= -\frac{d}{dr}(R_n)_{r=1} = -16\lambda_n^{3/2} e^{-2\lambda_n}\phi'(1-\lambda_n, 2; 4\lambda_n r^2)_{r=1}$$

$$= 8\lambda_n^{3/2}(\lambda_n - 1)e^{-2\lambda_n}\phi(2-\lambda_n, 3; 4\lambda_m r^2)_{r=1}$$

so that

$$b_n = \frac{\ell}{2K_n^2}\frac{(\lambda_n - 1)}{\lambda_n^{1/2}} e^{-2\lambda_n}\phi(2-\lambda_n, 3; 4\lambda_n) \qquad (n \le N) \tag{67}$$

The values of b_n were calculated manually from (67) and are shown in Table 3.

TABLE 3

THE COEFFICIENTS FOR THE ORTHOGONAL EXPANSION OF $\bar{v}_o(r)$

n	b_n
1	+1.086
2	-.9860
3	+.9276

4. Calculation of the Swirl Distribution

The swirl was calculated for several combinations of the parameters and various values of z^*, z, and r in the growth and decay regions. The specific combinations are shown in Table 4 and were also used in the experiments.

In Table 4, case A corresponds to swirl measurements made by Talbot [4] and the others to measurements made by the author. The various conditions were selected for the purposes of

a. gaining some idea of the highest value of for which the solution is sufficiently accurate for an investigation of stability,

b. testing the ability of the solution to account for changes in all the parameters , , and , including a point close to the line of incipient instability (= 1364, = .23), and

c. maintaining a laminar main flow by testing at values of the Reynolds number below the range in which there was any evidence of instability, due either to the swirl or to the shedding of eddies from the pipe entrance or from the boundary discontinuities.

TABLE 4

CONDITIONS FOR WHICH SWIRL WAS COMPUTED

Case	$\mathcal{R}$	$\mathcal{S}$	$\mathcal{L}$	z^*	z	r
A	861	.57	49.6		20	0, .1,--1.0
					40	"
					60	"
					90	"
B	861	.34	170.9	50		"
				100		"
				150		"
C	861	.34	170.9		20-90	"
D	1364	.23	170.9		20-90	"

Item c is discussed in more detail in the chapter describing the experiments.

The swirl profiles in the decay region are plotted in Figs. 4, 6, and 7 for cases A, C, and D.[3] Case B corresponds to Fig. 5 which is a plot of the swirl in the growth region for the same parametric values as for case C. The results of these plots are summarized in Fig. 8 where the swirl at a radius of .825 is plotted against axial position. This was the average radius of the oil drops used to measure the swirl velocity as these drops moved through the decay region.

[3]Figs. 4 through 8 contain plots of the exact

The swirl was determined by calculating the first three terms of the series solutions

$$v \cong \mathcal{L} r - \sum_{1}^{N} b_n R_n(r) e^{-\beta_n z^*} \qquad (0 < z^* < \ell) \tag{44}$$

$$v \cong \sum_{1}^{N} (1 - e^{-\beta_n \ell}) b_n R_n(r) e^{-\beta z} \qquad (0 < z) \tag{51}$$

The third term of the series was small or negligible for radii equal to and greater than those corresponding to maximum swirl. These radii are shown in Fig. 9. The radial interval in which the calculation is most accurate thus includes the point of maximum swirl and extends to the pipe wall. A solution which is accurate at small radii is not likely to be required in the analysis of the stability of swirling flow.

---

swirl solution, an approximate swirl solution, and measurements of the swirl. The approximate solution will be discussed in Chapter IV and the measurements in Chapter V. At present, the reader's attention is directed only to the exact solution which appears in Figs. 4 through 8 as an unbroken line.

CHAPTER IV

APPROXIMATE SOLUTION FOR THE SWIRL

1. Solution of the Swirl Equation by Successive Approximation Using Convergent Series

The exact shape of the radial profile of the swirl can be expected to be important for the analysis of stability [18]. In fact, it is later found that the swirl and its radial gradient appear in the stability equations. The need for accurate swirl profiles probably is greatest at large values of r where the radial gradient of angular momentum may be negative [27]. The swirl eigenfunctions, $R_n(r)$, are higher transcendental functions and possess a complicated combination of trigonometric and exponential characteristics. A simple approximation to the R_n would be desirable. However, asymptotic forms which were obtained, and which were nearly accurate as r approached one, were composed solely of exponential terms and gave unrealistic profiles for most of the range of r. Thus, the exact swirl solution of Chapter III may be required for analyzing stability, although a suitable approximation may be obtainable for reasons discussed in Chapter VI.

An approximate solution which provides a good description of gross characteristics, such as the maximum swirl, would be useful in some problems. One such solution has been

proposed [4]. Now that it can be compared with the exact solution obtained in the preceding chapter, it proves to be too inexact to be of value.

A considerably more accurate approximate solution will now be derived by a variation of the method used in [4] and credited to Heisenberg [18]. Assume a solution of the form

$$\bar{v} = \bar{R}(r)\, e^{-\bar{\beta} z} \tag{68}$$

Substitution in the swirl equation (27) yields

$$\frac{d^2\bar{R}}{dr^2} + \frac{1}{r}\frac{d\bar{R}}{dr} + \left[\mathcal{R}\bar{\beta}(1-r^2) - \frac{1}{r^2}\right]\bar{R} = 0 \tag{69}$$

Assume that $\bar{R}$ may be expanded in powers of a small-valued parameter ϵ, which is related to the parameter, $\mathcal{R}$.

$$\bar{R}(r) = \bar{R}_a(r) + \epsilon\bar{R}_b + \epsilon^2\bar{R}_c(r) + \cdots \tag{70}$$

and make the transformation

$$\eta = \frac{r}{\epsilon} \tag{71}$$

Substitution of (70) and (71) in (69) yields the equation

$$\left\{\bar{R}_a'' + \epsilon\bar{R}_b'' + \epsilon^2\bar{R}_c'' + \cdots\right\} + \frac{1}{\eta}\left\{\bar{R}_a' + \epsilon\bar{R}_b' + \epsilon^2\bar{R}_c' + \cdots\right\} + \left\{\mathcal{R}\bar{\beta}\epsilon^2(1-\eta^2\epsilon^2) - \frac{1}{\eta^2}\right\}\left\{\bar{R}_a + \epsilon\bar{R}_b + \epsilon^2\bar{R}_c + \cdots\right\} = 0 \tag{72}$$

If, as suggested by Lin [18] for a different problem, ϵ is chosen to be

(73) $$\epsilon = \frac{1}{\sqrt{R}}$$

the equations below are obtained by equating coefficients for each power of ϵ :

(74)
$$\epsilon^0: \quad \bar{R}_a'' + \frac{1}{\eta}\bar{R}_a' + (\bar{\beta} - \frac{1}{\eta^2})\bar{R}_a = 0$$

$$\epsilon^1: \quad \bar{R}_b'' + \frac{1}{\eta}\bar{R}_b' + (\bar{\beta} - \frac{1}{\eta^2})\bar{R}_b = 0$$

$$\epsilon^2: \quad \bar{R}_c'' + \frac{1}{\eta}\bar{R}_c' + (\bar{\beta} - \frac{1}{\eta^2})\bar{R}_c = -\bar{\beta}(\bar{\beta} - \eta^2)\bar{R}_a$$

$$\epsilon^n: \quad \bar{R}_n'' + \frac{1}{\eta}\bar{R}_n' + (\bar{\beta} - \frac{1}{\eta^2})\bar{R}_n = -\bar{\beta}(\bar{\beta} - \eta^2)\bar{R}_{n-2}$$

The solution of the first two of equations (74) which satisfies the homogeneous Dirichlet conditions

$$\bar{R}(0) = \bar{R}(1) = 0$$

required for the swirl function, is the Bessel function J_1, that is,

$$\bar{R}_a = \bar{R}_b = J_1(\sqrt{\bar{\beta}}\,\eta) = J_1(\sqrt{R\bar{\beta}}\,r)$$

Consequently, the solution of (69), correct to terms of order $R^{-\frac{1}{2}}$, is

(75) $$\bar{R}(r) = J_1(\sqrt{R\bar{\beta}_n}\,r)$$

where $\bar{\beta}_n$ are roots of

$$J_1\left(\sqrt{\mathcal{R}\bar{\beta}_n}\, r\right)_{r=1} = 0$$

The values of $\bar{\beta}_n$ prove to be in error by more than 25% as compared to the exact values β_n. This result might have been expected since (75) is a solution of

$$\frac{d^2\bar{R}}{dr^2} + \frac{1}{r}\frac{d\bar{R}}{dr} + \left[\mathcal{R}\bar{\beta} - \frac{1}{r^2}\right]\bar{R} = 0$$

so that, by comparison with (69), we have replaced $1-r^2$ by 1, a substitution which is accurate only for small r.

If, instead, we assume

(76) $$\epsilon = \frac{1}{\sqrt{K\mathcal{R}}}$$

the solution of (69) correct to terms of order $\mathcal{R}^{-\frac{1}{2}}$ is

(77) $$\bar{R} = J_1\left(\sqrt{K\mathcal{R}\bar{\beta}}\, r\right)$$

which is a solution of

$$\frac{d^2\bar{R}}{dr^2} + \frac{1}{r}\frac{d\bar{R}}{dr} + \left[K\mathcal{R}\bar{\beta} - \frac{1}{r^2}\right]\bar{R} = 0$$

where the function $1-r^2$ in (69) has been replaced by the constant k. To represent the gross characteristics of the swirl, we set

$$K = \frac{\int_0^1 (1-r^2)\,dr}{\int_0^1 dr} = \frac{2}{3}$$

whence the approximate swirl eigenfunction becomes

(78) $$\bar{R}(r) = J_1\left(\sqrt{\tfrac{2}{3}\mathcal{R}\bar{\beta}_n}\, r\right)$$

where $\bar{\beta}_n$ are the roots of

$$J_1\left(\sqrt{\tfrac{2}{3}\mathcal{R}\bar{\beta}_n}\, r\right)_{r=1} = 0$$

Setting

$$\mathcal{R}\bar{\beta}_n = 16\bar{\lambda}_n^2$$

we may compute the $\bar{\lambda}_n$ for the approximate eigenvalues and compare them with the exact values λ_n. The comparison is shown for five significant figures in Table 5 for n equal to one through 5.

It is seen that the first three values of the approximate axial decay parameter, $\bar{\beta}_n$, which in practice are usually sufficient for calculations, are correct within 3%. With respect to amplitude, the swirl eigenfunctions $R_1(r)$ and $J_1(\sqrt{\frac{2}{3}\mathcal{R}\bar{\beta}_1}\, r)$ are compared in Fig. 3. However, this comparison is best made by plotting the exact and approximate solutions for the swirl boundary problem, as will be done next.

2. The Approximate Solution of the Swirl Boundary Value Problem

In the same manner as described for the exact solution, the approximate solution of the swirl boundary value Problem, (27) through (35), is readily shown to be

TABLE 5

COMPARISON OF THE EXACT AND APPROXIMATE EIGENVALUES

n	λ_n	$\bar{\lambda}_n$	$\bar{\lambda}_n/\lambda_n$	$\bar{\beta}_n/\beta_n$
1	1.1560	1.1733	1.015	1.03
2	2.1619	2.1482	.994	.988
3	3.1638	3.1149	.985	.970
4	4.1646	4.0793	.980	.960
5	5.1651	5.0432	.976	.953

$$\bar{v} = \mathcal{A} r - \sum_{1}^{\infty} \bar{b}_n J_1\left(\sqrt{\tfrac{2}{3}\mathcal{K}\bar{\beta}_n}\, r\right) e^{-\bar{\beta}_n z^*} \qquad (0 < z^* < \ell) \tag{79}$$

$$\bar{v} = \sum_{1}^{\infty} \left(1 - e^{-\bar{\beta}_n \ell}\right) \bar{b}_n J_1\left(\sqrt{\tfrac{2}{3}\mathcal{K}\bar{\beta}_n}\, r\right) e^{-\beta_n z} \qquad (0 < z) \tag{80}$$

where the $\bar{b}_n$ are the coefficients of the usual Fourier-Bessel expansion and are such that

$$\sum_{1}^{\infty} b_n J_1\left(\sqrt{\tfrac{2}{3}\mathcal{K}\bar{\beta}_n}\, r\right) = v_0(r) \tag{81}$$

The solutions (79) and (80) were computed to three terms of the series in the growth and decay regions for cases B and C of Table 4. They are plotted in Figs. 5, 6, and 8 where they are seen to be in excellent agreement with the exact solution in the growth region. In the decay region, the approximate solution is seen to provide a good estimate of the maximum swirl except when z is small. The approximate solution does not provide an inflection point between the radius of maximum swirl and the wall as does the exact solution.

It is also considerably in error as to the magnitude and radial gradient of the swirl throughout the larger values of r, and it may provide too inaccurate a swirl profile shape to be of use in analyzing the stability.

CHAPTER V

EXPERIMENTATION

1. Introductory Remarks

The experimentation included a determination of the locus of values of the Reynolds number

$$\mathcal{R} = \frac{\bar{w}_m a}{\nu}$$

and the swirl parameter

$$\mathcal{S} = \frac{\Omega a}{\bar{w}_m}$$

corresponding to the onset of instability. The results of Talbot [4] and of the present work are shown in Fig. 2 for growth regions having lengths of 49.6 radii and 170.9 radii, respectively.

In addition, measurements were made of the swirl velocity for cases B, C, and D of Table 4 above. Case A represents the conditions for which swirl measurements were made by Talbot [4] and for which his data are available. The swirl velocity measurements are plotted in Figs. 4, 5, 6, 7, and 8.

2. Experimental Apparatus

The tests were conducted with a flow of water from an overhead tank which was equipped with an overflow weir to

provide a constant head. A vertical downtube led to a horizontal flow path. The latter consisted of a stilling chamber, rounded pipe entrance, and a straight pipe of cast lucite having a 1.25-inch inner diameter and an approximately 35-foot length. This length was divided as shown in Fig. 1 into an approach region of 13.1 feet (251 radii), a growth region (rotating section) of 8.9 feet (170.9 radii), and a decay region of about 13 feet. The stilling chamber contained a tube positionned coaxially with the lucite pipe. The tube had a capillary tip through which a suspension of dye or oil droplets could be introduced into the flow.

The pipe joints were lapped in order to provide a smooth continuous inner surface as the flow boundary. Sleeve bearings at the ends and center of the rotating section were similarly lapped and were counterbored at the outer ends in order to receive the adjacent sections of pipe. A variable-speed, electric drive was provided to turn the rotating section at the desired angular velocity.

The flow rate was measured by a precision-type, variable-area flowmeter which was reworked to obtain sensitivity to variations of the flow rate and insensitivity to variations of the viscosity or density of the water. The meter was calibrated directly in terms of the Reynolds number of the pipe. The angular velocity of the rotating section was measured with a revolution counter and stop watch, and the uniformity of the rotational speed was checked with a tachometer.

The equipment described was similar to that used in [4] with the exception of the instrumentation mentioned. Also, the available head was increased considerably and throttling valves were placed at the entrance to the stilling chamber and at the final outlet of the pipe. With these changes, and by adjusting the air space at the top of the stilling chamber, it was found possible to maintain a very steady rate of flow.

The Boussinesq relation is [13]

$$\frac{z_i}{2a} = 0.065\,\mathcal{R}$$

in which z_i is the required inlet length for the establishment of Poiseuille flow. The length of the approach region of 251 radii is found to be sufficient for all Reynolds numbers up to 1920. In the absence of swirl, the flow became turbulent at a Reynolds number of 3100. All measurements of swirl were conducted at Reynolds numbers of less than 1920, and all stability observations at values less than 3100.

3. Incipient Instability

For a growth region of 49.6 radii, Talbot [4] found a continuous locus of values of $\mathcal{R}$ and $\mathcal{S}$ corresponding to the onset of observable instability. This locus and that for the length of 170.9 radii are shown in Fig. 2. In all cases, the instability originated in the decay region at a dis-

tance z_c which increased with $\mathcal{R}$, as shown in Fig. 10.

With the longer rotating section, a smaller value of $\mathcal{L}$ was sufficient to produce instability at any given value of $\mathcal{R}$. The detailed character of the instability appeared to be unaffected by the length of the growth region and is summarized in Table 6 which includes the results of [4].

TABLE 6

INSTABILITY APPEARING IN THE DECAY REGION OF LAMINAR SWIRLING FLOW

$\mathcal{R}$	Instability
Less than 1800	Aperiodic sinuousity grew and then decayed until laminar flow returned.
1800 to 2500	Wavy sinuousity and turbulent bursts occurred over an axial range which lengthened with increase in $\mathcal{R}$ and was followed by laminar flow.
Greater than 2500	Eddies, periodic in r and z, became amplified with increase in z and led to fully developed turbulence.

The above data was obtained by observing a die filament introduced at the pipe entrance.

The appearance of spacially periodic eddies at the higher values of $\mathcal{R}$ suggests that laminar swirling flow is unstable in the decay region. However, the results in Table 6 are not conclusive evidence that such is the case. Except for moderate differences in the Reynolds numbers, the

description in Table 6 could be applied bodily to the behavior of a non-swirling laminar pipe flow in the inlet length following an abrupt or fairly rapid section reduction, as found by Schiller [7, pp. 323-324]. It has been proposed that in non-swirling pipe flow, the three types of instability described in Table 6 are due, respectively, to entrance conditions consisting of the following types [7]:

a. Separation at the entry produces a vortex sheet which reattaches to the pipe wall a short distance later. The sheet is unstable at low Reynolds numbers, resulting in the sinuousity at points farther downstream.

b. At intermediate values of the Reynolds number, still below 2100, the vortex sheet rolls up periodically and discrete eddies are formed.

c. As R approaches the critical value at which turbulent flow occurs, the vortex sheet rolls up into a single, large eddy which periodically casts off disturbance eddies.

The phenomenon of Table 6 occurred far downstream from the inlet length of Schiller and any disturbances due to the pipe entrance had decayed considerably before reaching the region of swirl decay. However, it is possible that a mechanism similar to that at a pipe entrance exists at the discontinuity of the boundary immediately preceding the decay region.

The stability of laminar swirling flow remains of interest, of course, especially in instances such as the Trans-Arabian oil pipeline where a discontinuity or rapid change in boundary conditions is absent and the mechanisms described in a, b, and c may not exist.

4. Measurement of the Swirl Velocity

The conditions under which the swirl velocity was measured have been set forth in Table 4. The results of the measurements are plotted in Figs. 4, 5, 6, 7, and 8 where they can be compared with the exact solution. The correlation is seen to improve with increase in R and decrease in the magnitude of the swirl. This result was suggested by order-of-magnitude considerations.

The swirl velocity was measured in the same manner as that employed in [4]. A mixture of mineral oil and alpha-chloronapthalene was prepared which had a specific gravity of about one. The mixture was dyed red with Sudan IV National Aniline fat staining dye. It was then mixed with water, violently agitated, and allowed to settle. Oil drops remaining in suspension for some length of time were then introduced into the flow at the pipe entrance by the centrally placed capillary tube.

The velocity data was obtained by photographing the drops as they passed a motion picture camera stationed at various axial positions. In calculating the velocities, use was made only of small axial and vertical displacements ofthe drops near the axis of the camera lens, which axis intersected that of the pipe. The radial positions of the drops were determined by comparing their axial velocities with that of Poiseuille flow. This radius and the vertical displacement were used to compute the arc length travelled by the drop during the time interval in question.

The camera was operated at an accurately known speed so that the time interval could be determined by counting frames. The data was corrected for the overall magnification of the lens of the camera and that of the projector used for studying the film.

The swirl velocity computed in this way tended to be too large due to the refraction of light by the fluid and walls of the pipe. The refraction error was measured for a radius of 0.825 and found to be +8% for the average vertical displacement observed, the latter being about 0.35-inch. This correction was applied to the data in Fig. 8 for α = .23. As a result, the measurements for low α substantiate the exact analytical solution.

It is interesting to note that the refraction error can be determined approximately from the swirl measurements in the growth region which are in Fig. 5 for α = .34. At a value of $z^* = 150$, the swirl had very nearly assumed rigid body rotation. The measured swirl at a radius of .825 should not exceed a value of .825 in the non-dimensional plot of Fig. 5. The height of the experimental point above the curve may thus be approximately the refraction error and indicates an error of about +6%.

The foregoing method of measuring velocity affords no control over the radii at which the oil drops came through the pipe. In practice, the mean radius was about .825 which is close to the inflection point of the radial distribution of the total swirl. For comparison, the first

harmonic of the swirl has an inflection point at a radius of .791. The concentration of the drops at large radii was noted also by Talbot [4] and is not fully understood. Lin [18] has shown that, in the parallel plane flow of an ideal fluid which is assumed to have vorticity, the inflection point of the transverse velocity distribution is a point of stable equilibrium for small eddies.

CHAPTER VI

THE HYDRODYNAMIC STABILITY PROBLEM FOR LAMINAR SWIRLING PIPE FLOW

1. The Equations of Hydrodynamic Stability for Laminar Swirling Pipe Flow

Order-of-magnitude considerations have been shown to suggest that, for a small swirl, the perturbation of the Poiseuille axial flow is probably small. In the case of swirl which is at most only moderately large, ($\mathcal{S} \leqq .23$), the exact solution for the swirl corresponds well with measurements, the reduction of which was based partially on the assumption of Poiseuille flow. For these reasons, we accept the dimensionless main flow in the decay region as being

(82) $$u \cong 0 \qquad (z>0)$$

(83) $$v \cong \sum_{1}^{N} (1-e^{-\beta_n \ell}) b_n R_n(r) e^{-\beta_n z} \qquad (z>0)$$

(84) $$w \cong 1-r^2 \qquad (z>0)$$

and, at large values of z, we take v as

(85) $$v \cong (1-e^{-\beta_1 \ell}) b_1 R_1(r) e^{-\beta_1 z} \qquad (z>>0)$$

The Navier-Stokes and continuity equations were seen earlier to be reducible to (10) and (11). If the several terms of the operator D_t are written out, (10) and (11) become

(86) $$\left[\frac{\partial}{\partial t} + u\frac{\partial}{\partial r} + w\frac{\partial}{\partial z} + \frac{u}{r} - \frac{1}{R}\textcircled{H}\right] v = 0$$

(87) $$\left[\frac{\partial}{\partial t} + u\frac{\partial}{\partial r} + w\frac{\partial}{\partial z} - \frac{u}{r} - \frac{1}{R}\textcircled{H}\right]\textcircled{H}\psi = -\frac{\partial}{\partial z}\left(\frac{v^2}{r}\right)$$

where

(88) $$\textcircled{H}\psi = \frac{\partial^2\psi}{\partial r^2} + \frac{1}{r}\frac{\partial\psi}{\partial r} - \frac{\psi}{r^2} + \frac{\partial^2\psi}{\partial z^2} \equiv \nabla_1^2\psi - \frac{\psi}{r^2} \equiv L(\psi) + \frac{\partial^2\psi}{\partial z^2}$$

In order to investigate the possibility of instability of the main flow due to self-excitation of initially small, random disturbances, we assume the presence of small perturbations of the main flow. In the majority of cases studied, three-dimensional disturbances which are rotationally symmetric have proven to be less stable than two-dimensional ones if the main flow was rotationally symmetric [43], [39], [18]. We therefore assume that the total perturbed flow is composed of

(89) $$u_T(r,z,t) = u(r,z) + u'(r,z,t)$$

(90) $$v_T(r,z,t) = v(r,z) + v'(r,z,t)$$

(91) $$w_T(r,z,t) = w(r,z) + w'(r,z,t)$$

and the total stream function is

(92) $$\psi_T(r,z,t) = \psi(r,z) + \psi'(r,z,t)$$

where

$$u = -\frac{1}{r}\frac{\partial(ru)}{\partial z} = -\frac{\partial \psi}{\partial z} \qquad u' = -\frac{1}{r}\frac{\partial(r\psi')}{\partial z} = -\frac{\partial \psi'}{\partial z}$$

(93)

$$w = \frac{1}{r}\frac{\partial(r\psi)}{\partial r} = \frac{\partial \psi}{\partial r} + \frac{\psi}{r} \qquad w' = \frac{1}{r}\frac{\partial(r\psi')}{\partial r} = \frac{\partial \psi'}{\partial r} + \frac{\psi'}{r}$$

which satisfy the continuity equation. The three-dimensional disturbances are represented by u', v', and w' or by v' and ψ'. These quantities are taken to be of equal order. The main flow components are the set u, v, and w or, alternately, the set v, ψ.

If the symbols u, v, w, and ψ represent the exact main flow, then these quantities satisfy the exact, non-linear Navier-Stokes equations (86) and (87). The total flow quantities on the left side of (89) through (92) must also satisfy (86) and (87). Substituting the total flow quantities (89) through (91) for the dependent variables in (86), and neglecting powers and products of the small disturbances and their derivatives (in comparison to corresponding linear disturbance-terms), we obtain

$$(94) \quad \frac{\partial v'}{\partial t} + u\frac{\partial v'}{\partial r} + u'\frac{\partial v}{\partial r} + w\frac{\partial v'}{\partial z} + w'\frac{\partial v}{\partial z} + u\frac{v'}{r} + u'\frac{v}{r} - \frac{1}{R}\textcircled{H}v' = 0$$

The main flow now is assumed to be given by (82), (83), and (84). Substituting (82), (84), and (93) in equation (94), we can write

$$(95) \quad \left[\frac{\partial}{\partial t} + (1-r^2)\frac{\partial}{\partial z} - \frac{1}{R}\textcircled{H}\right]v' = \frac{\partial \psi'}{\partial z}\left(\frac{\partial}{\partial r} + \frac{1}{r}\right)v - \left(\frac{\partial \psi'}{\partial r} + \frac{\psi'}{r}\right)\frac{\partial v}{\partial z}$$

Proceeding in the same manner, the substitution of (89) through (92) in (87) gives

$$(96)\quad \left[\frac{\partial}{\partial t}+u\frac{\partial}{\partial r}+w\frac{\partial}{\partial z}-\frac{u}{r}-\frac{1}{R}\textcircled{H}\right]\textcircled{H}\psi'+\left[u'\frac{\partial}{\partial r}+w'\frac{\partial}{\partial z}-\frac{u'}{r}\right]\textcircled{H}\psi=-\frac{2}{r}\frac{\partial}{\partial z}(vv')$$

When the main flow is taken as (82), (83) and (84), then in (96)

$$(97)\quad \textcircled{H}\psi=\frac{\partial w}{\partial r}-\frac{\partial u}{\partial z}=-2r$$

whence in (96) the quantity

$$(98)\quad \left[u'\frac{\partial}{\partial r}+w'\frac{\partial}{\partial z}-\frac{u'}{r}\right]\textcircled{H}\psi=u'(-2)+0-u'(-2)=0$$

Thus, the substitution of (82) and (84) in (96) results in

$$(99)\quad \left[\frac{\partial}{\partial t}+(1-r^2)\frac{\partial}{\partial z}-\frac{1}{R}\textcircled{H}\right]\textcircled{H}\psi'=-\frac{2}{r}\frac{\partial}{\partial z}(vv')$$

In arriving at equations (95) and (99), only the initial smallness of the disturbances and the magnitude of the main flow components have been employed for justifying linearization.

As the radial boundary conditions to be satisfied by the coupled, linear, partial differential equations (95) and (99), we select

$$(100)\quad \begin{aligned} &u'(0,z,t)=0 && u'(1,z,t)=0\\ &v'(0,z,t)=0 && v'(1,z,t)=0\\ &\frac{\partial w'}{\partial r}(0,z,t)=0 && w'(1,z,t)=0 \end{aligned}$$

In place of boundary, initial, and final conditions with respect to z and t, we assume the components of the disturbance to be periodic in the latter variables and hope that this condition will be sufficient to determine the secular equation uniquely.

Following the accepted practice [27, 18] we assume separated solutions of the form

$$\psi' = f(r)\, e^{i\alpha(z-ct)}$$
$$v' = g(r)\, e^{i\alpha(z-ct)} \tag{101}$$

If α is real and positive and r, z and c are complex, the forms (101) have the advantage that, if (with certain precautions) the linear system (95), (99), and (100) were solved for the complex functions ψ' and v', we could then let the imaginary parts of r and z go to zero and select as the solutions the real parts of the resulting expressions. Applying this process formally to (101), it is evident that the solutions would be of the forms

$$Re(\psi') = e^{\alpha c_i t}\left\{ f_r \cos(\alpha z - \alpha c_r t) - f_i \sin(\alpha z - \alpha c_r t)\right\}$$
$$= e^{\alpha c_i t}\left\{ \cos(\alpha z - \alpha c_r t + \epsilon_1)\right\}(f_r^2 + f_i^2)^{1/2}$$
$$Re(v') = e^{\alpha c_i t}\left\{ \cos(\alpha z - \alpha c_r t + \epsilon_2)\right\}(g_r^2 + g_i^2)^{1/2} \tag{102}$$
$$\epsilon_1 = \tan^{-1}\frac{f_i}{f_r}\ ; \qquad \epsilon_2 = \tan^{-1}\frac{g_i}{g_r}$$

The type of disturbance chosen in (101) is therefore very general. As seen in (102), the form selected may be considered the general term of a Fourier series in z. This series in turn can represent a wide class of disturbances because the form of each term is a traveling wave motion which is exponential and periodic in t and is arbitrary in r. The wave length is

$$\lambda = \frac{2\pi}{\alpha} \tag{103}$$

the celerity is c_r, the exponential time factor is αc_i, and ϵ is the phase angle of the amplitude oscillation with respect to the reference values of z and t.

In Taylor's study of the stability of Couette flow [43], the main flow differed from the present case in that

$$v = Ar + \frac{B}{r}$$
$$w = \frac{\partial v}{\partial z} = 0$$

whereas for laminar swirling flow we have

$$v = v(r, z)$$
$$w = 1 - r^2$$

When in (95) and (99) the quantities $1-r^2$ and $\frac{\partial v}{\partial z}$ vanish, and when v is given the form (Ar + B/r), then equations (95) and (99) reduce to the stability equations for Couette flow [27, p. 247].

2. Reduction of the Hydrodynamic Stability Equations to a Single Ordinary Differential Equation

The assumed form of disturbances, (101), permit reduction of the homogeneous, linear, partial differential system (95), (99), and (100) to a homogeneous, linear boundary value problem involving a single ordinary differential equation.

The two coupled equations (95) and (99) are first combined into a single equation. To do so, (95) is multiplied by the factor $(-\frac{2}{r}v)$ and subjected to the operation $\frac{\partial}{\partial z}$ to obtain

$$(104)\quad \left[\frac{\partial}{\partial t}+(1-r^2)\frac{\partial}{\partial z}-\frac{1}{R}\textcircled{H}\right]\cdot\left[-\frac{2}{r}\frac{\partial}{\partial z}(v'v)\right]$$
$$=-\frac{2}{r}\left[\frac{\partial^2\psi'}{\partial z^2}\left(\frac{1}{2}\frac{\partial}{\partial r}+\frac{1}{r}\right)v^2+\frac{\partial\psi'}{\partial z}\left(\frac{1}{2}\frac{\partial}{\partial r}+\frac{1}{r}\right)\frac{\partial}{\partial z}(v^2)\right.$$
$$\left.-\frac{1}{2}\left(\frac{\partial}{\partial r}+\frac{1}{r}\right)\frac{\partial\psi'}{\partial z}\frac{\partial}{\partial z}(v^2)-\frac{1}{2}\left(\frac{\partial\psi}{\partial r}+\frac{\psi}{r}\right)\frac{\partial^2}{\partial z^2}(v^2)\right]$$

where the use has been made of the relations

$$(105)\quad \textcircled{H}\left(\frac{1}{r}\right)=0$$

$$(106)\quad \left[\frac{\partial}{\partial t}+(1-r^2)\frac{\partial}{\partial z}-\frac{1}{R}\textcircled{H}\right]v(r,z)=0$$

To justify the latter equation, note that when $\frac{\partial^2 v}{\partial z^2}$ is of negligible order as shown in (26), (106) reduces to the swirl equation (27) of which v is a solution. Next, the operator on the left side of (104) is applied to (99) to obtain

$$(107)\quad \left[\frac{\partial}{\partial t}+(1-r^2)\frac{\partial}{\partial z}-\frac{1}{R}\textcircled{H}\right]^2\textcircled{H}\psi'=\left[\frac{\partial}{\partial t}+(1-r^2)\frac{\partial}{\partial z}-\frac{1}{R}\textcircled{H}\right]\left[-\frac{2}{r}\frac{\partial}{\partial z}(v'v)\right]$$

so that (104) and (107) combine to give

$$(108) \qquad \left[\frac{\partial}{\partial t} + (1-r^2)\frac{\partial}{\partial z} - \frac{1}{R}\textcircled{H}\right]^2 \textcircled{H}\psi' = P$$

where P is the right side of (104).

The disturbance forms (101) can now be substituted into (108) to obtain, in a straightforward manner, the following single equation for the hydrodynamic stability of laminar swirling pipe flow:

$$(109) \qquad \left[-\alpha^2(1-r^2-c)^2 - \frac{2i\alpha}{R}(1-r^2-c)(2-\alpha^2) + 3\frac{i\alpha}{R} + \frac{1}{R^2}(2-\alpha^2)^2\right](2-\alpha^2)f$$

$$= -\frac{2}{r}\left[-\alpha^2 f\left(\frac{1}{2}\frac{\partial}{\partial r}+\frac{1}{r}\right)v^2 + i\alpha f\left(\frac{1}{2}\frac{\partial}{\partial r}+\frac{1}{r}\right)\frac{\partial(v^2)}{\partial z} - \frac{i\alpha}{2}\frac{\partial(v^2)}{\partial z}\left(\frac{\partial}{\partial r}+\frac{1}{r}\right)f - \frac{1}{2}\frac{\partial^2(v^2)}{\partial z^2}\left(\frac{\partial}{\partial r}+\frac{1}{r}\right)f\right]$$

At this point a difficulty arises in that (109) possesses no solution in separated form, as is easily seen when forms (83) or (85) are substituted for v. The difficulty arises from the fact that, unlike most previous stability studies, here the main flow has z-dependence. To circumvent this problem, we arbitrarily adopt the method of Tatsumi [28] and study the stability of a family of z-independent main flows corresponding to the actual main flow in the decay region at various values of z. Thus, replace z by the parameter z_o in (85) and (109), and discard the terms on the right side of (109) which contain $\frac{\partial}{\partial z}$ and $\frac{\partial^2}{\partial z^2}$. These steps yield the following single stability equation:

$$(110)\quad \left[-\alpha^2(1-r^2-c)^2-\frac{2i\alpha}{\mathcal{R}}(1-r^2-c)(L-\alpha^2)+\mathcal{J}\frac{i\alpha}{\mathcal{R}}+\frac{1}{\mathcal{R}^2}(L-\alpha^2)^2\right](L-\alpha^2)f(r)$$
$$= 2\frac{\alpha^2}{r}v(r,z_0)\left[v'(r,z_0)+\frac{v(r,z_0)}{r}\right]f(r)$$
$$= \frac{\alpha^2}{r^3}\frac{\partial}{\partial r}\left\{\left[rv(r,z_0)\right]^2\right\}f(r)$$

in which

$$v(r,z_0)\cong(1-e^{-\beta_1\ell})b_1R_1(r)e^{-\beta_1 z_0}\qquad(z_0>0)$$

and $v(r,z_0)$ has been obtained from (85).

Equation (110) is a complex, homogeneous, linear, sixth-order, ordinary differential equation with dependent variable f, independent variable r, and parameters $\mathcal{R}$, $\mathcal{S}$, ℓ, α, c, and z_0. $\mathcal{S}$, ℓ, and z_0 are contained in the swirl term v and the other parameters appear explicitly in (110). The quantities f(r) and c are complex by definition. If it is convenient during the course of the solution of (110) to allow r to assume complex values, the swirl eigenfunction $R_1(r)$, will become complex. Since it was shown earlier to be an analytic function for all finite r, its complex swirl form is uniquely determined by analytic continuation and will be an entire function of r.

From (100) and (101), the sufficient boundary conditions on f(r) are readily determined to be

$$(111)\quad f(0)=0 \qquad f(1)=0 \qquad [u']$$

$$(112)\quad L[f(0)]=0 \qquad f'(1)+f(1)=0 \qquad [w']$$

$$(113)\quad L^2[f(0)]=0 \qquad \frac{1}{R_1(1)}L^2[f(1)]=0 \qquad [v']$$

where conditions (113) assume that (111) and (112) have been satisfied. Conditions (113) were obtained by applying (85) and the boundary conditions (100) to equation (95).

3. Discussion of the Stability Problem

The hydrodynamic stability problem (110) through (113) is more complicated than those solved previously. The additional complications arise from the z-dependence of the main flow, the highly transcendental nature of the eigenfunctions which express the radial-dependence of the swirl, and the probable necessity for assuming three-dimensional disturbances. No attempt will be made here to solve the problem. However, certain properties of the solutions can be obtained which indicate that, in principle, the type of approach which has been refined by Lin [18], Tollmein [31], Pekeris [22], Morawetz [21], Wasow [32], and DiPrima [16] for the stability of parallel, planar flows gives promise of successful application here. Since the statement of the problem in equations (110) through (113) has been carefully derived in light of the experience in solving planar flows of the parallel and curved types, the chances are favorable that the solution will have physical significance. However, there is no guarantee that such will be the case and experimental verification will ultimately be necessary.

Further work with the system (110) through (113) may indicate that stability results useful in ordinary pipelines

require that the swirl solution substituted for v in (110) should be obtained for an initial radial distribution (at z = 0) which is continuous. In the present case, the swirl possesses a maximum radial gradient which approaches negative infinity at a value of r which approaches unity as z approaches zero from positive values. We may avoid this difficulty mathematically by using (85) in place of (83), but the former is inaccurate near z = 0. However, these matters do not affect the following discussion for which we require only that v behave well enough so that if it becomes complex it will be an entire function of r. It has been shown in Appendix I that an orthogonal expansion of the swirl eigenfunctions has this property when the swirl at z equal to zero is sufficiently well-behaved, as would be the case for mathematical models of practical problems which do not have boundary discontinuities.

The tangential velocity component (swirl) of the main flow enters equation (110) as a coefficient of the zero order derivative of the independent variable. Inspection of (110) reveals that the swirl and its first derivative with respect to r are factors in the stability but that the second derivative is unimportant. This situation may permit the development of a simple, approximate, closed-form solution for the swirl which accurately represents the exact swirl function and its first derivative. Alternately, (110) indicates that the stability is affected by the

radial gradient of the square of the angular momentum of the main flow. This is exactly the form in which the main flow enters the stability equations for Couette flow [27, p. 247]. Here, it was found that a necessary, but not sufficient, condition for instability is that the radial gradient of the angular momentum be negative. A similar showing for the present problem would signify that the swirl can be unstable only in the decay region.

Regardless of the initial conditions, it is apparent from the solution of the swirl equation in the decay region will be of the form

$$v \cong \sum_{1}^{N} d_n(\mathcal{A}, \ell) R_n(r) e^{-\beta_n z_0} \qquad (z_0 > 0) \tag{114}$$

where $\beta_n = \frac{16\lambda_n^2}{\mathcal{R}}$

Consequently, the complex equation (110) has at most singularities at zero values of r and at infinite values of r, $\mathcal{R}$, α , and c. Its complex solutions are then entire functions of the parameters $\mathcal{R}$, α , and c. $\mathcal{A}$, ℓ , and z_0 also fall in this category when the swirl is generated as in Fig. 1.

The six linearly independent solutions, f_j, of (110) possess, at most, singularities at r = 0 for the interesting range of r which is the interval (0, 1). The general solution of (110) will be of the form

$$f = \sum_{j=1}^{M} A_j f_j(\mathcal{R}, \alpha, c, \mathcal{L}, \ell, z_0, r) \tag{115}$$

where M is a maximum of 6 and will be less than this by that portion of the six solutions which have singularities at a zero value of r. This fact is a simplifying feature not present for parallel flows. The condition that the unkown constants A_j exist is the usual determinantal equation

$$\begin{vmatrix} f_1(0) & f_2(0) & - & - & - & f_6(0) \\ f_1(1) & - & - & - & - & - \\ L[f_1(0)] & - & - & - & - & - \\ - & - & - & - & - & - \\ - & - & - & - & - & - \\ \frac{1}{R_1(1)} L^2[f(1)] & - & - & - & - & - \end{vmatrix} = 0 \tag{116}$$

which, when expanded, provides a complex secular equation

$$F(\mathcal{R}, \alpha, c, \mathcal{L}, \ell, z_0) = 0 \tag{117}$$

Based on the preceding discussion, the function F is an entire function of the complex parameter c. Equation (117) may therefore be solved for c.

If c_r and c_i are the real and imaginary parts of c, write the two equations

$$c_r = c_r(\mathcal{R}, \alpha, \mathcal{L}, \ell, z_0) \tag{118}$$

$$c_i = c_i(\mathcal{R}, \alpha, \mathcal{L}, \ell, z_0) \tag{119}$$

By equation (101), the condition for neutral stability is

$$c_i(\mathcal{R}, \alpha, \mathcal{L}, \ell, z_0) = 0 \tag{120}$$

It is then convenient to assign interesting values to the parameters $\mathcal{K}$ and ℓ and determine the minimum values of $\mathcal{L}$ for which (120) is satisfied when α and z are greater than zero. The result can be plotted as in Fig. 2 with $\mathcal{K}$ and $\mathcal{L}$ as the axes and ℓ as the parameter.

CHAPTER VII

CONCLUSIONS AND RECOMMENDATIONS

1. Concluding Remarks

The rotationally symmetric Navier-Stokes equations, linearized by assuming Poiseuille axial flow and negligible radial flow, have an exact solution for the swirl in laminar pipe flow. The actual flow can be made to approach the assumed conditions by decreasing the swirl, that is, increasing the Reynolds number ($\mathcal{R}$) of the axial flow, decreasing the swirl parameter ($\mathcal{S}$), or decreasing the length ($\mathcal{L}$) of the rotating section. As $\mathcal{R}$ was increased and $\mathcal{S}$ was decreased at a given value of $\mathcal{L}$, the exact solution converged to the results of measurements of the swirl which were made at large values of z^*, z, and r. At small values of the latter quantities, the solution is probably not so accurate.

The eigenfunctions expressing the radial dependence of the exact solution for the swirl are complicated. They include the product of an exponential factor and a form of the confluent hypergeometric function. The eigenvalues appear as a parameter in several ways, being a factor of the argument in both parts of the product and also appearing in the parameter of the numerator in the general term for confluent hypergeometric function. However, the swirl

eigenfunctions prove to have all the necessary properties to permit satisfying the radial and axial boundary conditions occurring in pipe flow when the velocity field is everywhere continuous. Furthermore, they may be used to form solutions of problems containing discontinuous boundary conditions, at least when the discontinuities are limited to distinct null regions such as separated circumferential lines.

The approximate solution in terms of Bessel functions gives a useful description of the gross characteristics of the swirl in both the growth and decay regions.

Interesting types of instability are observed in the region where the swirl decays, especially for values of R above 1800 where periodic eddies appear. In this range, the corresponding values of α are very small and those of z are large. The first harmonic of the exact solution, together with the assumed Poiseuille axial flow, therefore can be expected to give a description of the main flow which is sufficiently accurate to be used in the analysis of the stability problem. The existence of swirl instability was not shown conclusively in the present work because the observations were made under ambiguous circumstances due to the presence of a boundary discontinuity at the beginning of the decay region. The discontinuous boundary did have the value of verifying the main flow analysis under drastic conditions.

The mathematical formulation of the stability problem governing the self-excitation of small disturbances is readi-

ly accomplished. The resulting differential system has properties similar to those for main flows which are parallel and planar. The methods of solution developed for the latter flows should be applicable in principle to the present case. The stability problem includes a sixth-order differential equation in which the swirl enters in precisely the same manner as in the case of Couette flow. The sixth-order stability equation reduces to that for Couette flow when the latter is taken as the main flow.

2. Recommendation for Further Work

Future work should be both theoretical and experimental. The swirl solution has been verified sufficiently to justify an attempt to solve the stability problem. However, the solution of stability problems inherently involves assumptions as to the form of disturbances and, when the process is completely analytic, many approximations are required. Also, it is necessary to assume whether the mechanism leading to observable instability is one of resonance or self-excitation. Consequently experiments on the stability of laminar swirling pipe flow are needed to test the assumptions and approximations of the theoretical analysis. Tests should be devised which avoid discontinuities in the boundary conditions and other unrealistic circumstances. At the present writing no good scheme for achieving such conditions has been conceived, mainly because no concerted effort has yet been expended in this direction.

There is need for an improved method of measuring the velocity distribution of the laminar swirling flow. The method used here gives reasonably good results but only with excessive and tedious work. Furthermore, it affords no positive control over the radial position at which the velocity is measured. While this lack need not delay the study of the stability of swirling flow, a superior technique for measuring velocity is necessary for a more detailed check of the swirl solution. Also, it is a pressing need in the field of viscous flow research. Here, analytic solutions are required because they afford insight not supplied by numerical solutions. In order to obtain them, the non-linear Navier-Stokes equations usually must be solved by approximate methods containing debatable assumptions, and the need for experimental verification is especially great.

APPENDIX I

THE PROPERTIES OF THE SWIRL EIGENVALUES AND EIGENFUNCTIONS

The analysis below is presented in some detail because it provides an efficient procedure for ascertaining the properties of boundary value problems which are singular cases of the general theory. This situation can occur quite frequently in hydrodynamics where a wide variety of new differential systems can arise, depending on the manner in which the non-linear Navier-Stokes equations are reduced to meet the circumstances of each problem.

The swirl function R(r) is a solution of the homogeneous, linear boundary value problem

(I-1) $$\frac{d^2R}{dr} + \frac{1}{r}\frac{dR}{dr} + \left[16\lambda_n^2(1-r^2) - \frac{1}{r^2}\right]R = 0$$

(I-2) $$R(0) = 0$$

(I-3) $$R(1) = 0$$

where the parameter λ of (I-1) also proves to be contained in R(r). If multiplied by r, equation (I-1) may be put in the self adjoint form

(I-4) $$\frac{d}{dr}\left[r\frac{dR}{dr}\right] + \left[16\lambda^2 r(1-r^2) - \frac{1}{r}\right]R = 0$$

This equation with the boundary conditions (I-2) and (I-3) has the form of a special case of the Sturm-Liouville system. The general theory [50, 235] for such a system guarantees the existence of an infinite set of orthogonal and complete eigenfunctions, such as R_n, provided certain conditions are met. The latter include the requirement that the coefficients in (I-4) be continuous in the closed interval

$$0 \leq r \leq 1$$

This condition is not met in the case of the coefficient $\frac{1}{r}$ of (I-4). The stipulations of the general theorem also include the requirement that the coefficients r and $r(1-r^2)$ be greater than zero in the closed interval, which condition is satisfied by neither of these quantities. In view of this failure of the theory of differential equations to provide a convenient analysis of the problem, we shortly resort to the theory of integral equations.

It is desired to prove principally that there exist eigenfunctions R_n of the real variable r which are orthogonal and are also complete with respect to the initial conditions $\bar{v}_o(r)$ of the swirl problem. Specifically, it is desired to show that there exist constants b_n such that at least for finite values of N,

(I-5) $$\sum_1^N b_n R_n(r) \cong \bar{v}_o(r)$$

where

(I-6) $$b_n = \frac{1}{K_n^2}\int_0^1 r(1-r^2)\,\bar{v}_o(r)R_n(r)\,dr = \frac{1}{K_n^2}\int_0^1 r(1-r^2)\,rR_n(r)\,dr$$

$$\bar{v}_0(r) = \alpha r \quad (0 \le r < 1)$$
$$= 0 \quad (r = 1)$$

(I-7)

$$K_n^2 = \int_0^1 r(1-r^2) R_n^2(r)\, dr$$

The equality in (I-5) means that the coefficients b_n are those for which the series converges to $\bar{v}_0(r)$ in the mean, identically, or, at least, are those for which partial sums of it closely approximate $\bar{v}_0(r)$. In the first case, the b_n are those for which the series (I-5) provides the best approximation to $\bar{v}_0(r)$ in the sense of least squares. That is,

$$I = \int_0^1 \left[\sum_1^N b_n R_n(r) - \bar{v}_0(r)\right]^2 dr$$

is a minimum when the b_n are given by (I-6). The method of proof used below is suggested under different circumstances in [1] and [54]. In these references, the initial conditions are assumed to be analytic instead of having the discontinuous behavior (I-7) which is required here. We now prove the validity of equation (I-5) for the condition (I-7).

The linear, homogeneous system (I-1) through (I-3) may be written

$$r\frac{d^2R}{dr^2} + \frac{dR}{dr} - \frac{1}{r} = -16\lambda^2 r(1-r^2)R$$

(I-8)

$$R(0) = R(1) = 0$$

It has been noted that solutions of (I-8) are analytic for all finite r and λ. Consider the right side of (I-8) to be an inhomogeneous term $f(r)$. The corresponding homogeneous problem is then

$$r\frac{d^2R}{dr} + \frac{dR}{dr} - \frac{1}{r^2} = 0$$

(I-9)

$$R(0) = R(1) = 0$$

This system is incompatible in that neither of the two linearly independent solutions

$$\frac{1}{r}, \; r$$

of the differential equation, nor the general solution

$$Ar + \frac{B}{r}$$

is capable of satisfying $R(0) = R(1) = 0$. Under these circumstances the Green's function, $G(r, \xi)$, of the system (I-8) exists [50, p. 254]. Then

(I-10) $$R = -16\lambda^2 \int_0^1 G(r, \xi)\, \xi(1-\xi^2) R(\xi)\, d\xi$$

is a solution of the swirl boundary value problem (I-8). The Green's function is readily shown to be

(I-11) $$G(r, \xi) = \frac{1-r^2}{2r}\xi \qquad (0 \le \xi \le r)$$

$$= r\frac{1-\xi^2}{2\xi} \qquad (r \le \xi \le 1)$$

Equation (I-10) is a homogeneous Fredholm integral equation of the second kind with the kernel $\left[\xi(1-\xi^2) G(r, \xi)\right]$. Multiplying equation (I-10) by $\left[r(1-r^2)\right]^{1/2}$ leads to

(I-12) $$\left[r(1-r^2)\right]^{1/2} R(r)$$

$$= -16\lambda^2 \int_0^1 \left\{\left[\xi r(1-\xi^2)(1-r^2)\right]^{1/2} G(r, \xi)\right\} \left[\xi(1-\xi^2)\right]^{1/2} R(\xi)\, d\xi$$

or

$$R^*(r) = -16\lambda^2 \int_0^1 K(r,\xi)\, R^*(\xi)\, d\xi \qquad \text{(I-13)}$$

where

$$R^*(r) = [r(1-r^2)]^{1/2} R(r)$$

$$K(r,\xi) = \xi r(1-\xi^2)(1-r^2)\, G(r,\xi)$$
$$= \tfrac{1}{2}\xi^2(1-\xi^2)(1-r^2)^2 \qquad (0 \le \xi \le r)$$
$$= \tfrac{1}{2} r^2 (1-\xi^2)^2 (1-r^2) \qquad (r \le \xi \le 1)$$

By inspection, equation (I-13) is therefore, a homogeneous Fredholm equation of the second kind with a singular but integrable kernel, $K(r,\xi)$, which is real, quadratically integrable, bounded, positive-definite, and symmetric with respect to inversion of r and ξ. Consequently, the following properties are assured [54, p. 913].

a. The function $R^*(r)$, which is directly related to solutions of the swirl problem (I-10), is a solution of (I-13) only when λ assumes discrete values λ_n, the eigenvalues.

b. The λ_n^2 are real, possibly infinite in number, and form a monotonically increasing sequence with a positive lower bound. (Lauwerier [51] has shown that the sequence is an infinite one.)

c. The functions $R^*(r)$, corresponding to the various eigenvalues λ_n, are denoted $R_n^*(r)$ and referred to as the eigenfunctions of the kernel $K(r,\xi)$. They form an orthogonal set.

d. The set $R_n^*(r)$ is complete with respect to $K(r,\xi)$

and may therefore be used to form an orthogonal expansion which converges to $K(r,\xi)$ at least in the mean and possibly identically.

In order to show that $R_n(r)$ may be the basis for an orthogonal expansion which represents $\bar{v}_o(r)$, select a function $\bar{\bar{v}}_o(r)$ which is related to $\bar{v}_o(r)$ but is better behaved, such as,

$$\bar{\bar{v}}_o(r) = (r - r^m)\mathcal{L} \tag{I-14}$$

where m is a constant which is real and greater than three. Replacing R(r) in (I-8) by $\bar{\bar{v}}_o(r)$, form the inhomogeneous boundary value problem

$$r\frac{d^2\bar{\bar{v}}_o}{dr^2} + \frac{d\bar{\bar{v}}_o}{dr} - \frac{\bar{\bar{v}}_o}{r} = -r^{m-1}(m^2-1)\mathcal{L} \tag{I-15}$$

$$\bar{\bar{v}}_o(0) = \bar{\bar{v}}_o(1) = 0$$

where we temporarily suppose $\bar{\bar{v}}_o(r)$ to be an unknown solution of (I-15). The corresponding homogeneous problem is incompatible as was the case for (I-8). Thus by comparison of (I-8) and (I-15) we have the analogous quantities

$$\bar{\bar{v}}_o(r) \sim R(r) \tag{I-16}$$

$$-r^{m-1}(m^2-1)\mathcal{L} \sim -16\lambda^2 r(1-r^2)R(r)$$

so that for problem (I-15) the relation corresponding to (I-12) is

$$\left[r(1-r^2)\right]^{1/2}\bar{\bar{v}}_o(r) = \int_0^1 \left\{r(1-r^2)\,G(r,\xi)\right\}\left[-\xi^{m-1}(m^2-1)\mathcal{L}\right]d\xi \tag{I-17}$$

$$= \int_0^1 K(r,\xi)\frac{-\xi^{m-1}(m^2-1)}{\left[\xi(1-\xi^2)\right]^{1/2}}\mathcal{L}\,d\xi$$

which is a Fredholm integral equation of the first kind with the well-behaved kernel already described. By definition $\mathscr{A}$ is a predetermined constant and not an arbitrary constant such as λ . We demand solutions of (I-17) good for any value of $\mathscr{A}$.

Since the function $\bar{\bar{v}}_o(r)$ in equation (I-14) satisfies $\bar{\bar{v}}_o(0) = \bar{\bar{v}}_o(1) = 0$, and since its first three derivations are continuous in the closed interval (0, 1), it may be shown that the coefficient of $K(r,\xi)$ in (I-17) is quadratically integrable. Under such a circumstance [53], the function on the left side of (I-17) may be represented identically, or at least in the mean, by the following absolutely and uniformly convergent series of the orthogonal eigenfunctions, R_n^* , of the kernel $K(r,\xi)$. That is,

$$\left[r(1-r^2)\right]^{1/2}\bar{\bar{v}}_o(r) = \sum_1^\infty B_n R_n^*(r) = \sum_1^\infty B_n \left[r(1-r^2)\right]^{1/2} R_n(r)$$

or

$$\bar{\bar{v}}_o(r) = \sum_1^\infty B_n R_n(r) \cong \sum_1^N B_n R_n(r) \tag{I-18}$$

where the last series approaches $\bar{\bar{v}}_o(r)$ uniformly in r as N is increased, and where

$$B_n = \frac{1}{K_n^2}\int_0^1 \left[r(1-r^2)\right]^{1/2}\bar{\bar{v}}_o(r)\left[r(1-r^2)\right]^{1/2} R_n(r)\,dr \tag{I-19}$$

$$= \frac{\mathscr{A}}{K_n^2}\int_0^1 r(1-r^2)(r-r^m)\,R_n(r)\,dr$$

Also,

$$K_n^2 = \int_0^1 r(1-r^2)\,R_n^2(r)\,dr \tag{I-20}$$

At least when the λ_n are finite, the solutions R_n of the boundary problem (I-8) are analytic in (0,1). Also,

$$\lim_{m\to\infty} r^m = \begin{cases} 0 & (0 \le r < 1) \\ 1 & (r = 1) \end{cases}$$

Therefore,

$$\lim_{m\to\infty} B_n = \frac{\mathcal{A}}{K_n^2} \int_0^1 r(1-r^2)\, r R_n(r)\, dr = b_n \qquad (n \le N) \tag{I-21}$$

Furthermore,

$$\lim_{m\to\infty} \bar{\bar{v}}_0(r) = \lim_{m\to\infty} (r - r^m)\mathcal{A} = \begin{cases} \mathcal{A}r & (0 \le r < 1) \\ 0 & (r = 1) \end{cases}$$

so that

$$\lim_{m\to\infty} \bar{\bar{v}}_0(r) = \bar{v}_0(r)$$

Consequently, if m becomes arbitrarily large, equation (I-18) summed to N approaches

$$\bar{v}_0(r) \cong \sum_1^N b_n R_n(r) \tag{I-22}$$

where

$$b_n = \frac{\mathcal{A}}{K_n^2} \int_0^1 r(1-r^2)\, r R_n(r)\, dr \qquad (n \le N) \tag{I-23}$$

and (I-20) remains unchanged by the limiting process.

If the series in (I-22) converges rapidly to $\bar{v}_0(r)$, the result shown in equation (I-22) will be satisfactory. In fact, for the stability problem it is highly desirable to have a finite number of terms which describe $\bar{v}_0(r)$ accurately. The restriction that

$$n \leqq N < \infty$$

in (I-21) and (I-22) is made because the swirl equation in the separated form (37) has a singular point at λ equal to infinity. This singularity is pertinent because the λ_n extend to infinity so that the swirl eigenfunctions, R_n, may become singular in (0, 1) as n increases indefinitely. This point has never been investigated [49, pp. 280-282] and its analysis is very complicated. Consequently, the limit given in (I-21) can be guaranteed to hold only when N is finite and the series (I-22) may diverge when summed to infinity.

The clarification of this matter requires the asymptotic form of $\phi(1-\lambda_n, 2; 4\lambda_n r^2)$ as λ_n approaches infinity. The difficulty in obtaining such a form stems from the fact that for all values of r greater than zero both the parameter $(1-\lambda_n)$ and argument $(4\lambda_n r^2)$ approach infinity (in absolute value) as n increases. The asymptotic form has not been obtained for the present case where the parameter of the numerator $(1-\lambda_n)$ is negative and non-integral, and the parameter of the denominator (two) is a positive integer.

Even the divergence of (I-22) could be beneficial, however, because partial sums of divergent series often converge closely to a given function (such as $\bar{v}_o$) before diverging as still further terms are added. The convergence is frequently more rapid than in convergent infinite series, so that in practice divergent expansions can be very useful [54, p. 554]. The only question here is the

rapidity with which (I-22) approaches $\bar{v}_0(r)$ as N is increased. The first three terms of (I-22) were calculated. As n was increased to three, they decreased monotonically and alternated in sign and their sum quickly approached $\bar{v}_0(r)$, as shown in Fig. 11. It was concluded that (I-22) with N = 3 was a good approximation to $\bar{v}_0(r)$, because when the swirl was computed from

(I-24) $$v = \sum_{1}^{3} \left(1 - e^{-\beta_n \ell}\right) b_n R_n(r) e^{-\beta_n z} \qquad (0 < z)$$

for the plots in Figs. 4, 6, 7, and 8, the third term was less than 4% of the sum of three terms and the probable error due to partial summation was less than 1% for the following ranges of the independent variables

$$20 \leq z$$

$$[r]_{v_{max.}} \leq r \leq 1$$

The discussion in Chapters V and VI indicates these ranges to be those in which instability of the swirling flow is most likely to occur.

The finite series (I-22) is absolutely and uniformly convergent in the strict sense of these terms. The possibility remains that it converges absolutely and uniformly when summed to infinity, and that it then converges to $\bar{v}_0(r)$ identically or at least in the mean. In any case, the eigenfunctions may be used to form orthogonal expansions which converge in the above manner to well-behaved radial distributions of the swirl at the initial value of z. Specifically, expansions such as (I-18) will converge in the above manner to functions which are as well-behaved as $\bar{\bar{v}}_0(r)$.

APPENDIX II

CONDITIONS FOR SMALL DEVIATION OF THE AXIAL VELOCITY FROM POISEUILLE DISTRIBUTION

The deviation, w_2, from Poiseuille distribution of the axial velocity component in swirling flow, was estimated by Talbot [4] at various axial positions in the decay region. In particular, a momentum-integral method was used and w_2 was calculated approximately for one pair of values of the Reynolds number ($\mathcal{R}$) and the swirl parameter ($\mathcal{S}$). In this appendix, necessary conditions for w_2 to be small in both the growth and decay regions will be determined. The method used is different from that employed in [4].

The solution of the swirl problem which is given in Chapter III was obtained from the linearized form of equation (10). In order to obtain the conditions for w_2 to be small, equation (11) will now be linearized by means of the same magnitude assumptions as those employed in reducing (10). These assumptions are as follows:

$$\frac{\partial}{\partial r} = O(1)$$

$$\frac{\partial}{\partial z} = O(\epsilon^{-1}) \qquad \text{(II-1)}$$

$$w(r,z) = w_1(r) + w_2(r,z)$$

$$w_1(r) = 1 - r^2 = \Theta(1)$$

(II-2)

$$w_2(r,z) = \Theta(-2)$$

$$u(r,z) = \Theta(-3)$$

The order of u follows from the assumed order of w_2 by the argument which immediately preceded equation (24) and for which only the assumption (II-1) was required. The order of v remains unspecified.

Equation (11) is here written as

(II-3) $$\left[u\frac{\partial}{\partial r} + w\frac{\partial}{\partial z} - \frac{u}{r} - \frac{1}{R}\textcircled{H}\right]\textcircled{H}\psi = -\frac{1}{r^2}\frac{\partial}{\partial z}(v^2)$$

(II-4) $$u = -\frac{\partial \psi}{\partial z} \qquad w = \frac{\partial \psi}{\partial r} + \frac{\psi}{r}$$

(II-5) $$\textcircled{H}\psi = \left(L + \frac{\partial^2}{\partial z^2}\right)\psi = \frac{\partial w}{\partial r} - \frac{\partial u}{\partial r}$$

The radial boundary conditions for a rotationally-symmetric flow of a viscous liquid in a pipe of radius one are

$$u(0,z) = 0 \qquad u(1,z) = 0$$

(II-6)

$$\frac{\partial w}{\partial r}(0,z) = 0 \qquad w(1,z) = 0$$

In terms of ψ, these conditions are

$$\psi(0,z) = 0 \qquad \psi(1,z) = 0$$

(II-7)

$$L[\psi(0,z)] = 0 \qquad \frac{\partial}{\partial r}[\psi(r,z)]_{r=1} + \psi(1,z) = 0$$

The orders of the quantities appearing in (II-3) are

$$\textcircled{H}\psi = \frac{\partial w}{\partial r} - \frac{\partial u}{\partial z} = \frac{\partial w_1}{\partial r} + \frac{\partial w_2}{\partial r} - \frac{\partial u}{\partial z} = O(1) + O(-2) + O(-4)$$

$$u\frac{\partial}{\partial r}\textcircled{H}\psi = u\left(\frac{\partial^2 w_1}{\partial r^2} + \frac{\partial^2 w_2}{\partial r^2} - \frac{\partial^2 u}{\partial z\,\partial r}\right) = O(-3) + O(-5) + O(-7)$$

$$w\frac{\partial}{\partial z}\textcircled{H}\psi = (w_1 + w_2)\left(\frac{\partial^2 w_2}{\partial z\,\partial r} - \frac{\partial^2 u}{\partial z^2}\right) = O(-3) + O(-5) + O(-5) + O(-7)$$

$$\frac{u}{r}\textcircled{H}\psi = \frac{u}{r}\left(\frac{\partial w_1}{\partial r} + \frac{\partial w_2}{\partial r} - \frac{\partial u}{\partial z}\right) = O(-3) + O(-5) + O(-7)$$

The last term on the left side of (II-3) is

$$\frac{1}{R}\textcircled{H}\left[\textcircled{H}\psi\right] = \left[L + \frac{\partial^2}{\partial z^2}\right]\left(\frac{\partial w_1}{\partial r} + \frac{\partial w_2}{\partial r} - \frac{\partial u}{\partial r}\right)$$

in which

$$\frac{1}{R}L\left(\frac{\partial w_1}{\partial r}\right) = \frac{1}{R}L(-2r) = 0$$

$$\frac{1}{R}\frac{\partial^2}{\partial z^2}\left(\frac{\partial w_1}{\partial r}\right) = \frac{1}{R}\frac{\partial^2}{\partial z^2}(-2r) = 0$$

$$\frac{1}{R}L\left(\frac{\partial w_2}{\partial r}\right) = \frac{1}{R}O(-2)$$

$$\frac{1}{R}L\left(\frac{\partial u}{\partial z}\right) = \frac{1}{R}O(-4)$$

$$\frac{1}{R}\frac{\partial^2}{\partial z^2}\left(\frac{\partial w_2}{\partial r}\right) = \frac{1}{R}O(-4)$$

$$\frac{1}{R}\frac{\partial^2}{\partial z^2}\left(\frac{\partial u}{\partial z}\right) = \frac{1}{R}O(-6)$$

If only the largest terms of (II-3) are retained, this equation becomes

$$u\frac{\partial}{\partial r}\left(\frac{\partial w_1}{\partial r}\right)+w_1\frac{\partial}{\partial z}\left(\frac{\partial w_2}{\partial r}\right)-\frac{u}{r}\left(\frac{\partial w_1}{\partial r}\right)-\frac{1}{\mathcal{R}}\mathcal{L}\left(\frac{\partial w_2}{\partial r}\right)=\frac{-1}{r}\frac{\partial}{\partial z^2}(v^2) \tag{II-8}$$

When

$$w_1 = 1-r^2$$

the terms

$$u\frac{\partial}{\partial r}\left(\frac{\partial w_1}{\partial r}\right)-\frac{u}{r}\left(\frac{\partial w_1}{\partial r}\right)=u\left[-2-(-2)\right]=0$$

so that equation (II-8) may be written

$$\left[\frac{\partial^2}{\partial r^2}+\frac{1}{r}\frac{\partial}{\partial r}-\mathcal{R}(1-r^2)\frac{\partial}{\partial z}-\frac{1}{r^2}\right]\frac{\partial w_2}{\partial r}=\frac{\mathcal{R}}{r}\frac{\partial}{\partial z}(v^2)$$

or

$$\frac{\partial}{\partial r}\left[w_{2rr}+\frac{w_{2r}}{r}\right]-\mathcal{R}(1-r^2)\frac{\partial}{\partial z}w_{2r}=\frac{\mathcal{R}}{r}\frac{\partial}{\partial z}(v^2) \tag{II-9}$$

in which

$$w_{2r} \equiv \frac{\partial w_2}{\partial r}$$

Only terms in u have been dropped. Thus only the first of the assumptions (II-1) and (II-2) has been used in obtaining (II-9). In particular, the latter equation is not dependent on the assumption that

$$w_2 = O(-2)$$

In both the growth and decay regions, equation (II-9) is subject to the radial boundary conditions

$$w_{2r}(0,z)=0 \qquad w_2(1,z)=0 \tag{II-10}$$

and the continuity condition

(II-11) $$\int_0^1 r\, w_z(r,z)\, dr = 0$$

Equation (II-9) will now be integrated over the interval (0, 1). Because solutions of the problem (II-9), (II-10), and (II-11) are analytic for all z on the infinite, real, positive axis, we shall take some liberties in interchanging the order of integration with respect to r and differentiation with respect to z. Then (II-9) becomes

(II-12) $$w_{zrr}\Big]_0^1 + \frac{w_{zrr}}{r}\Big]_0^1 - \kappa\frac{\partial}{\partial z}\left[w_z\right]_0^1 + \kappa\frac{\partial}{\partial z}\left[r^2 w_z\right]_0^1 - \kappa\frac{\partial}{\partial z}\int_0^1 2r w_z\, dr = \frac{\kappa}{r}\int_0^1 \frac{\partial}{\partial z}(v^2)\, dr$$

If (II-9) is multiplied by r and the latter is allowed to vanish, there results

(II-13) $$\lim_{r\to 0}\left[\frac{w_{zr}}{r}\right] \equiv \frac{w_{zr}}{r}\Big]_{r=0} = w_{zrr}(0,z)$$

The substitution of (II-10), (II-11), and (II-13) in equation (II-12) results in

(II-14) $$w_{zrr}(1,z) - 2w_{zrr}(0,z) + w_{zr}(1,z) + \kappa\frac{\partial}{\partial z}w_z(0,z) = \frac{2\kappa}{r}\int_0^1 v\frac{\partial v}{\partial z}\, dr$$

The component w_2 is a perturbation of the Poiseuille flow. Appropriate changes in the parameters $\mathcal{K}$, $\mathcal{A}$, and $\mathcal{L}$ which decrease w_2 will ultimately make the left hand side of (II-14) arbitrarily small. The integral on the right hand side must behave similarly. Because v does not change sign in the radial interval (0, 1), the result

(II-15) $$\lim_{w_2 \to 0} \left| v \frac{\partial v}{\partial z} \right|_{max} \to 0$$

is a necessary condition that w_2 become small.

Because only the radial boundary conditions on w_2 have been considered and the axial ones disregarded, (II-15) applies in both the growth and decay regions of the swirl. It is contingent only upon the applicability of the boundary-layer approximation

$$\frac{\partial}{\partial z} < \frac{\partial}{\partial r}$$

which was justified on physical grounds. It is always possible that the factor $\frac{\partial v}{\partial z}$ will be large in some regions, as in the present problem in the neighborhood of the boundary discontinuities. Consequently a necessary condition for w_2 to be small in the growth and decay regions is that v be small, say at least as small as

(II-16) $$v = O(-1)$$

For the present problem in particular, the swirl in the decay region is given by

(II-17) $$v \cong \mathcal{A} \sum_{1}^{N} \left(1 - e^{-\frac{16\lambda_n^2}{\mathcal{K}}\mathcal{L}}\right)\left(\frac{b_n}{\mathcal{A}}\right) P_n(r)\, e^{-\frac{16\lambda_n^2}{\mathcal{K}}z} \qquad (0 < z)$$

where λ_n and $\frac{b_n}{\mathcal{A}}$ are constants independent of the parameters $\mathcal{K}$, $\mathcal{A}$, and $\mathcal{L}$. Equation (II-16) will be satisfied if

(II-18)
a. $\mathcal{K}$ is increased sufficiently,
b. $\mathcal{A}$ is decreased sufficiently, or
c. $\mathcal{L}$ is decreased sufficiently

When the form (II-17) is substituted in (II-15), it is seen that the parameters $\mathcal{K}$, $\mathcal{A}$, and $\mathcal{L}$ are effective as their squares so that changes in the directions described in (II-18) may be expected to cause rapid decrease in w_2.

BIBLIOGRAPHY

The Rate of Decay of Swirl in Pipe Flow

1. COLLATZ, L., and GÖRTLER, H. Rohrströmung mit schwachem Drall. ZAMP 5: 95-110. 1954.

2. FORTIER, A. Damping out the rotation and head losses of gyratory pipe flows in straight pipelines of circular section. Houille Blanche 9, B: 670-675. 1954.

3. HENRICI, P. On rotational viscous flow through a tube. ZAMP 5: 511-516. 1954.

4. TALBOT, L. Laminar Swirling Pipe Flow. J. appl. Mech. 21: 1-7. 1954.

5. WUNDT, H. Decay of small swirl superimposed on laminar flow in a circular tube. ZAMP 5: 270-276. 1954.

General References

6. ASHLEY, H., and HAVILAND, G. Bending vibrations of a pipe line containing flowing fluid. J. appl. Mech. 72: 229-232. 1950.

7. GOLDSTEIN, S. (ed.). "Turbulent flow between rotating cylinders." Modern Developments in Fluid Mechanics. Oxford University Press, London, 1938.

8. HOUSNER, G. W. Bending vibrations of a pipeline containing flowing fluid. J. appl. Mech. 19: 205-208. 1952.

9. KOLIN, A. Demonstration of parabolic velocity distribution in laminar flow. Am. J. Phys. 21: 619-620. 1953.

10. LONG, R. H. Experimental and theoretical Study of transverse vibrations of a tube containing flowing

fluid. ASME Ann. Meet., N. Y., 1954. Pap. 54-A22, 4 pp.

11. MICHE, R. Détermination par un principe variationnel du mouvement non lent des fluides visqueux. Application aux houles du large. Revue General de l'Hydraulique 41: 227-236. 42: 295-300. 1947.

12. NIORDSON, F. I. Vibrations of a cylindrical tube containing flowing fluid. Kungl. Tekniska Hogskolans Handlingar 73: 1-27. 1953.

13. PRANDTL, L., and TIETJENS, O. G. Applied Hydro- and Aeromechanics. McGraw-Hill Book Co., Inc., New York. 1934.

14. REYNOLDS, O. An experimental investigation of the circumstances which determine whether the motion of water shall be direct or sinuous and the law of resistance in parallel channels. Phil. Trans., Roy. Soc., London 174: 935. 1883.

The Stability of Parallel Plane Flows

15. CORCOS, G. M. On the Stability of Poisuille Flows. Ph. D. Thesis, University of Michigan. 1952.

16. DI PRIMA, R. C. A Note on the Asymptotic Solutions of the Equation of Hydrodynamic Stability. J. Math. Phys. 33: 249-257. 1954.

17. HEISENBERG, W. Über Stabilität und Turbulenz von Flüssigkeitsströmen Ann. d. Phys., Lpz. 74: 577-627. 1924.

18. LIN, C. C. On the stability of two-dimensional parallel flows. Quart. appl. Math. 3: 117-142, 218-234, 277-301. 1945.

19. _____. Some physical aspects of the stability of parallel flows. Proc. Nat. Acad. Sci., Wash. 40: 741-747. 1954.

20. _____. The Theory of Hydrodynamic Stability. Cambridge University Press, Cambridge. 1955.

21. MORAWETZ, C. S. The eigenvalues of some stability problems involving viscosity. J. Rat. Mech. Anal. 1: 579-603. 1952.

22. PEKERIS, C. L. Stability of laminar flow through a straight pipe of circular cross section to infinitesimal disturbances which are symmetrical about the axis of the pipe. Proc. Nat. Acad. Sci., Wash. 34: 285-295. 1948.

23. PRANDTL, L. Article in Aerodynamic Theory, edited by W. F. Durand 3: 178-190. Julius Springer, Berlin. 1935.

24. SCHUBAUER, G. B. and SKRAMSTAD, H. K. Laminar Boundary Layer Oscillations on a Flat Plate. NACA TR 909, 13 pp., 1955.

25. SELLARS, J. R. Some Special Problems in the Stability of Laminar Flows. Ph. D. Thesis, University of Michigan. 1952.

26. SQUIRE, G. B. On the stability of the three dimensional disturbances of viscous fluid flow between parallel walls. Proc. Roy. Soc. A 142: 621-628. 1933.

27. SYNGE, J. L. "Hydrodynamical Stability." Semi-Centennial Publications of the Amer. Math. Soc. 2 (Addresses): 227-269. 1938.

28. TATSUMI, T. Stability of the laminar inlet-flow prior to the formation of Poisuille Regime. I, II. J. Phys. Soc. Japan 7: 489-495, 495-502. 1952.

29. TAYLOR, G. I. Statistical theory of turbulence. V. Effect of turbulence on the boundary layer. Proc. Roy. Soc. A 156: 307-317. 1936.

30. _____. Some recent developments in the study of turbulence. Proc. 5th Int. Congr. Appl. Mech., Cambridge, U. S. A., 1933.

31. TOLLMEIN, W. Asymptotische Integration der Störungs-differentialgleichung ebener laminar Strömungen bei hohen Reynoldschen Zahlen. ZAMM 25: 33-50. 1947.

32. WASOW, W. Asymptotic solution of the differential equation of hydrodynamic stability in a domain containing a transition point. Ann. of Math. 58: 222-253. 1953.

33. YIH, C. On small disturbances of plane couette flow. U. S. Nat. Bu. Stds. J. of Res. 51: 195-202. 1953.

34. _____. Stability of parallel laminar flow with a free surface. Proc. 2nd U. S. Nat. Congr. Appl. Mech., N. Y., 1954. 623-628.

35. _____. Stability of two-dimensional parallel flows for three-dimensional disturbances. Quart. appl. Math. 12: 434-435. 1955.

The Stability of Curved Plane Flows

36. DEAN, W. R. Fluid motion in a curved channel. Proc. Roy. Soc. A 121: 402-420. 1928.

37. FAXEN, H. Konvergenz Untersuchungen zu G. I. Taylors Abhandlung über die Stabilität der Bewegungen einer zähen Flüssigkeit zwischen zwei rotierenden Zylindern. Ark. Mat. Astr. Fys. 21A: 1-11. 1928.

38. GORTLER, H. Über den Einfluss der Wandkrummung auf die Enstehung der Turbulenz. ZAMM 20: 138-147. 1940.

39. _____. Über eine dreidimensionale Instabilität laminarer Grenzschichten an konkaven Wanden. Nachr. Ges. Wiss. Göttingen, N. F. 2: 1-26. 1940.

40. HARRISON, W. J. On the stability of the steady motion of viscous liquid contained between rotating coaxial cylinders. Proc. Camb. Phil. Soc. 20: 455-459. 1921.

41. SCHLICHTING, H. Über die Enstehung der Turbulenz in einem rotierendem Zylinder. Nachr. Ges. Wiss. Göttingen. Math-Phys. Klasse: 160-168. 1932.

42. TAMAKI, K., and HARRISON, W. J. On the stability of the steady motion of viscous liquid contained between two rotating coaxial circular cylinders. Trans. Camb. Phil. Soc. 22: 425-448. 1920.

43. TAYLOR, G. I. Stability of a viscous liquid contained between two rotating cylinders. Phil. Trans., Roy. Soc. Lond. 223: 289-343. 1923.

The Stability of Non-Planar Flows

44. FAGE, A. The influence of wall oscillations, wall rotation, and entry eddies on the breakdown of laminar flow in an annular pipe. Proc. Roy. Soc. A 165: 513-517. 1938.

45. GOLDSTEIN, S. The stability of viscous fluid flow between rotating cylinders. Proc. Camb. Phil. Soc. 33: 46-61. 1937.

Mathematical References

46. ADAMS, E. P., and HIPPISLEY, R. L. Smithsonian Mathematical Formulae and Tables of Elliptic Functions. Smithsonian Institution, Washington. 1922.

47. British Association for the Advancement of Science Reports, 45th Meeting, Leeds, England, 1927. p. 220.

48. BUCHHOLZ, H. Die konfluente hypergeometrische Function. Springer-Verlag, Berlin. 1953.

49. ERDÉLYI, A. et al. Higher Transcendental Functions, Vol. 1. McGraw-Hill Book Co., Inc., New York. 1953.

50. INCE, E. L. Ordinary Differential Equations. First American Edition. Dover Publications, New York. 1944.

51. LAUWERIER, H. A. The use of the confluent hypergeometric functions in mathematical physics and the solution of an eigenvalue problem. Appl. Sci. Res. A 2: 184-204. 1950.

52. MACDONALD, A. D. Tables of the Function $e^{-qz/r} M(\alpha, \beta, z)$ Tech. Rpt. No. 130, Mass. Inst. of Tech.: 1-10. 1949.

53. MCLACHLIN, N. W. Bessel Functions for Engineers. 2nd Ed. Oxford University Press, London. 1955.

54. MORSE, P. M. and FESHBACH, H. Methods of Theoretical Physics. Vol. 1 and 2. McGraw-Hill Book Co., Inc., New York. 1953.

55. SNEDDON, I. N. Fourier Transforms. McGraw-Hill Book Co., Inc., New York. 1951.

56. SZEGO, G. Orthogonal Polynomials. Amer. Math. Soc. Colloquium Public. 23, N. Y., 1939.

57. TITCHMARSH, E. C. Eigenfunction Expansions Associated with Second-Order Differential Equations. Oxford University Press, London. 1946.

58. WATSON, G. N. A Treatise on the Theory of Bessel Functions. 2nd Ed. Cambridge University Press, Cambridge. 1944.

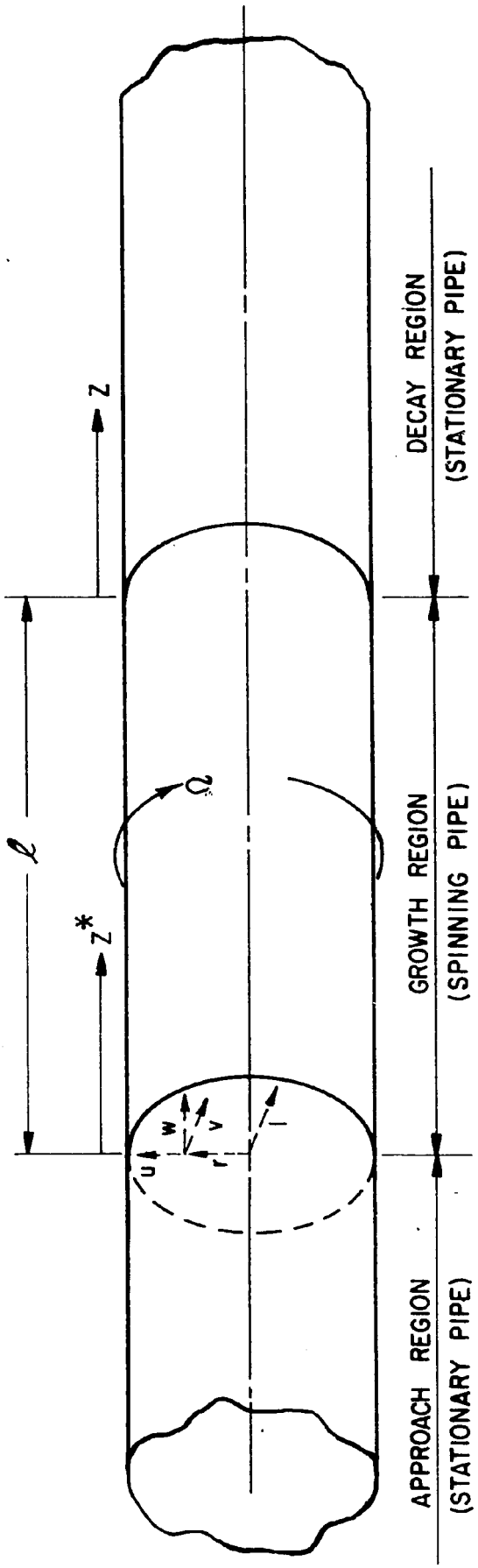


Fig. 1. - FLOW BOUNDARIES, CO-ORDINATE SYSTEM, AND VELOCITY NOTATION

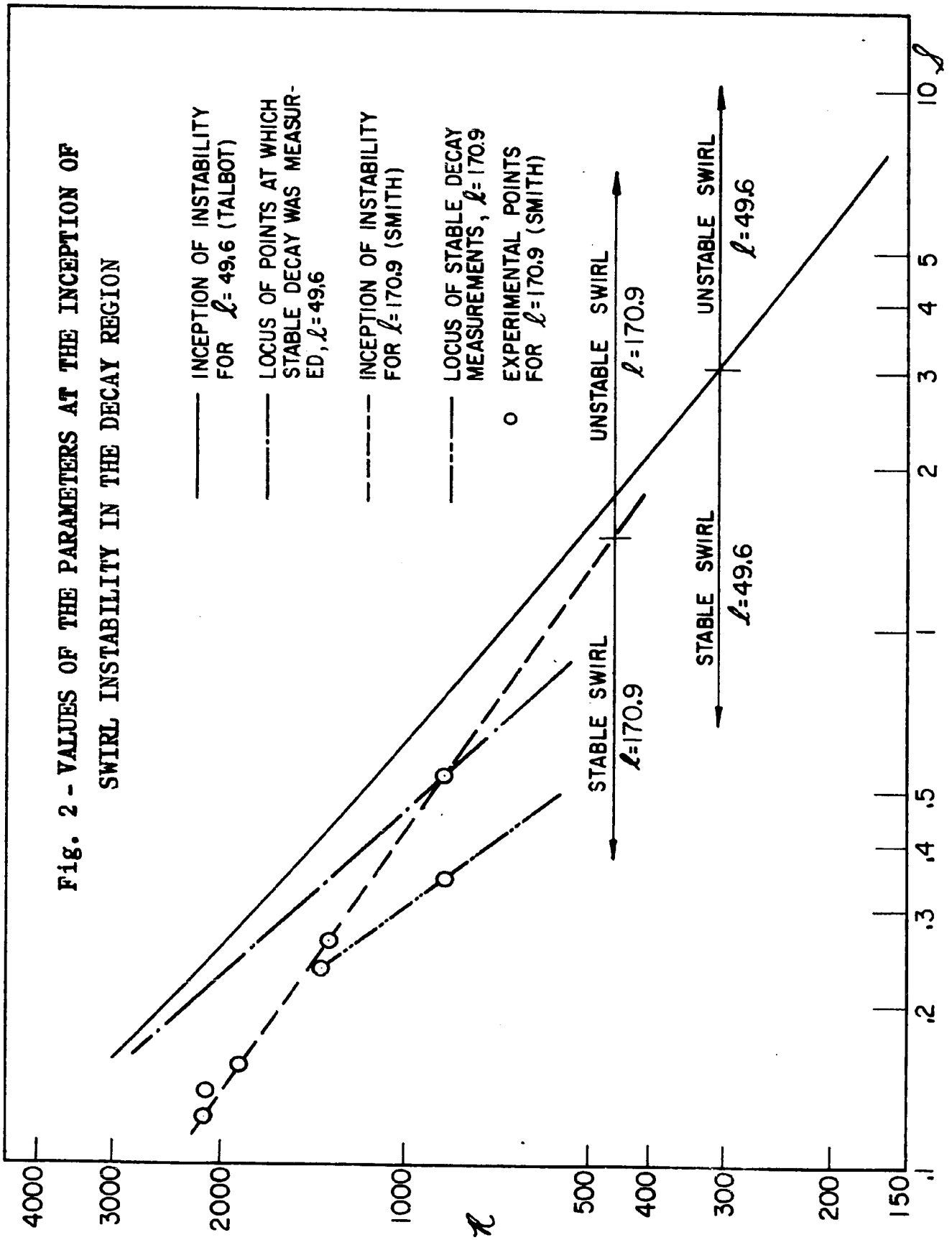
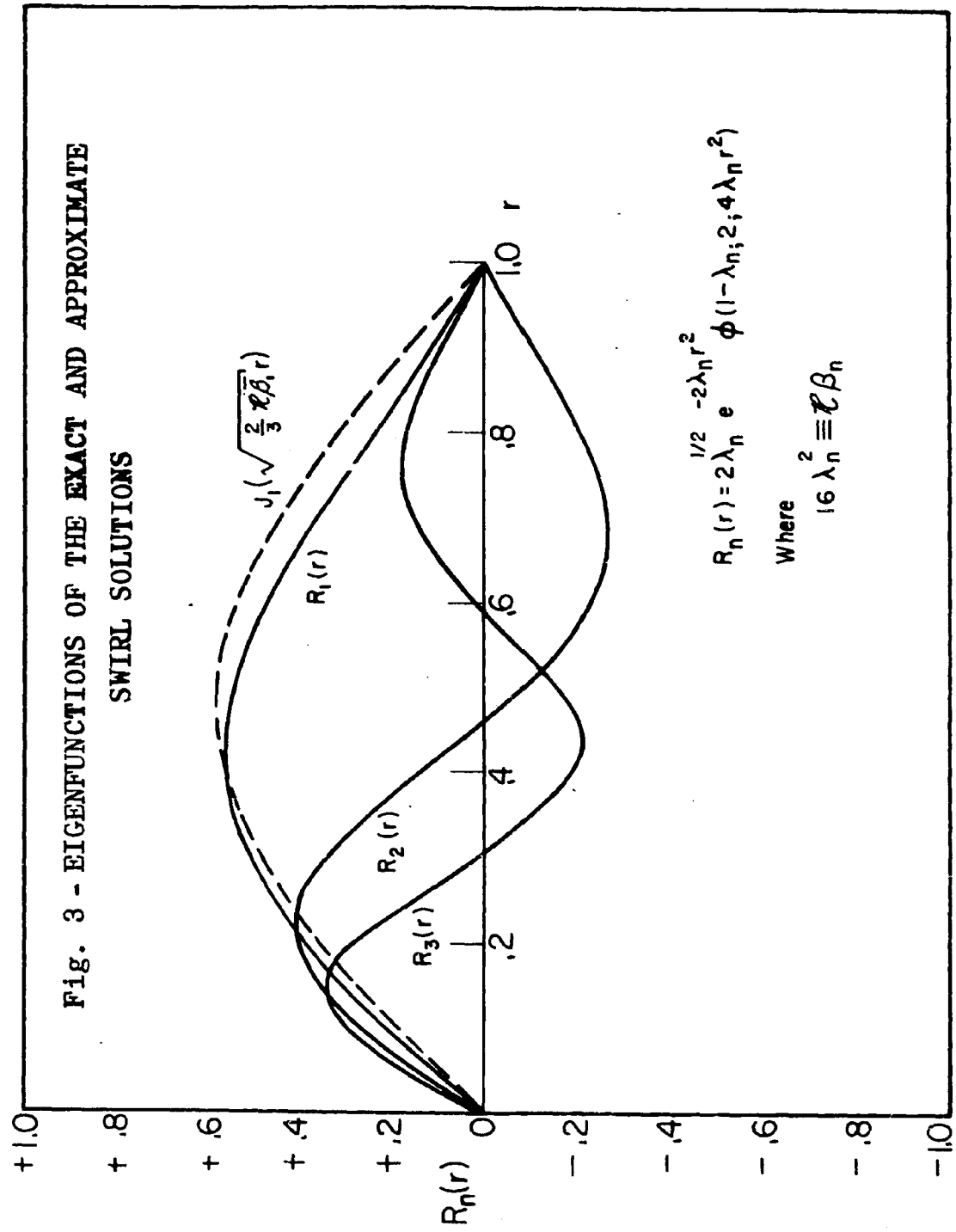
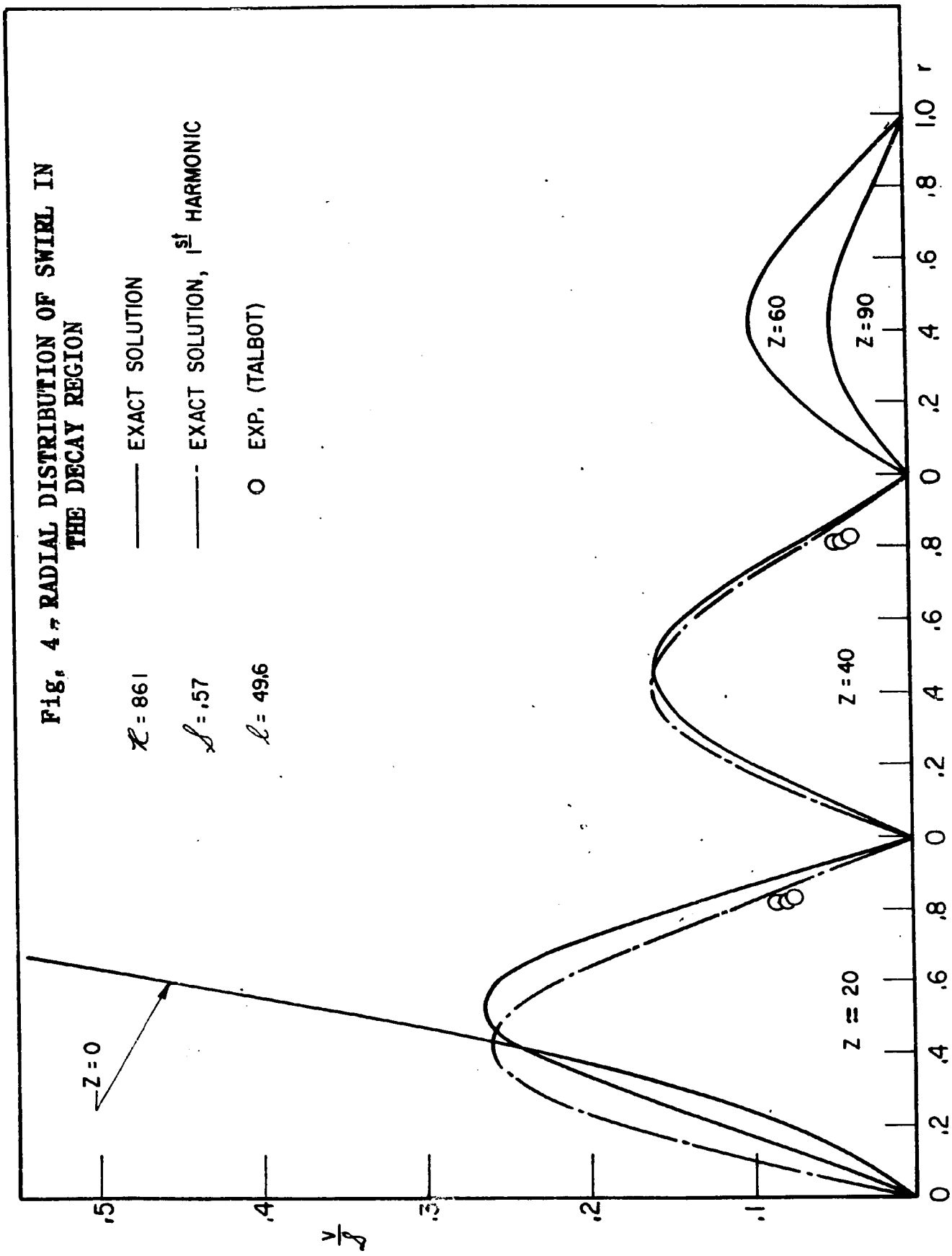
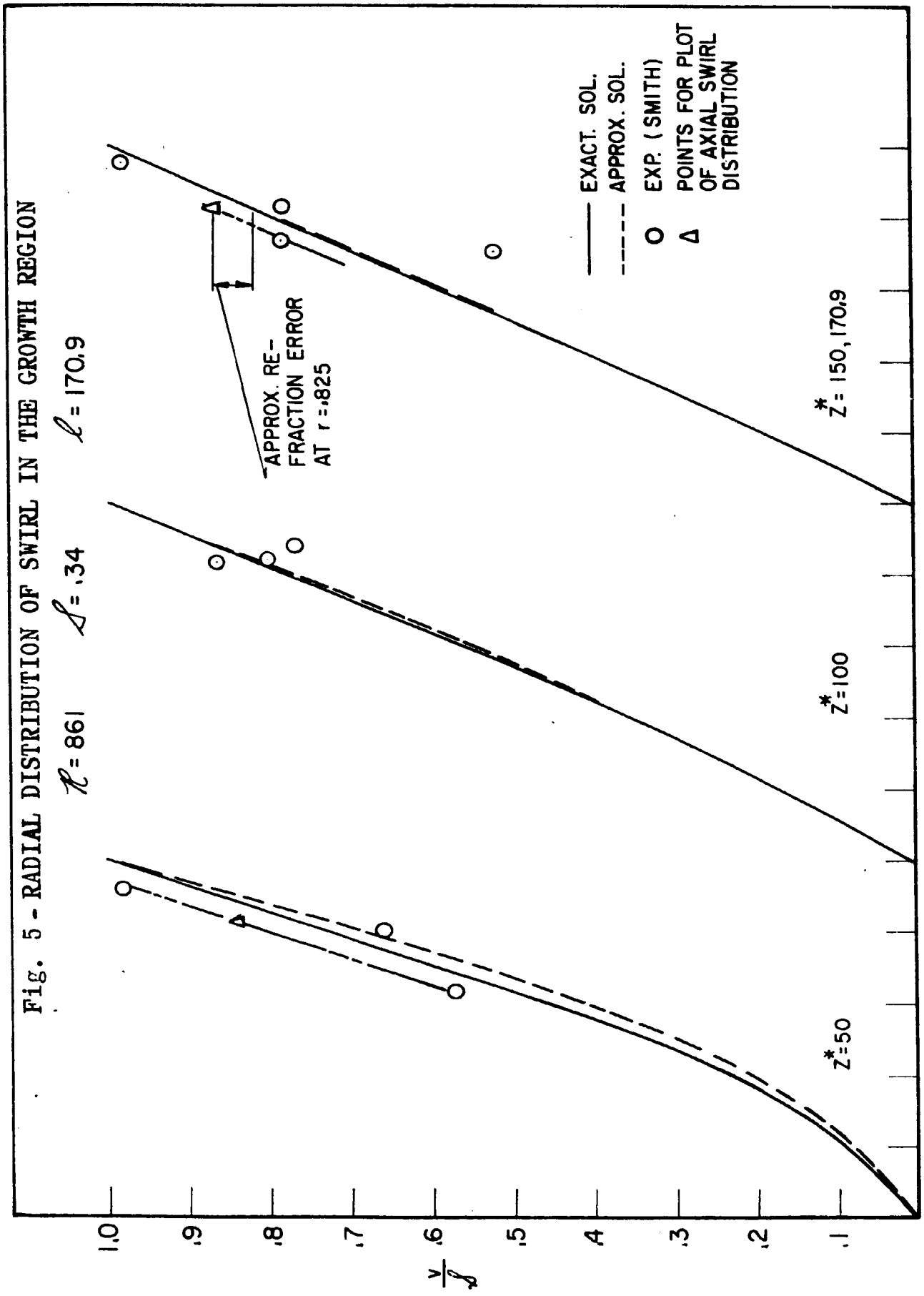
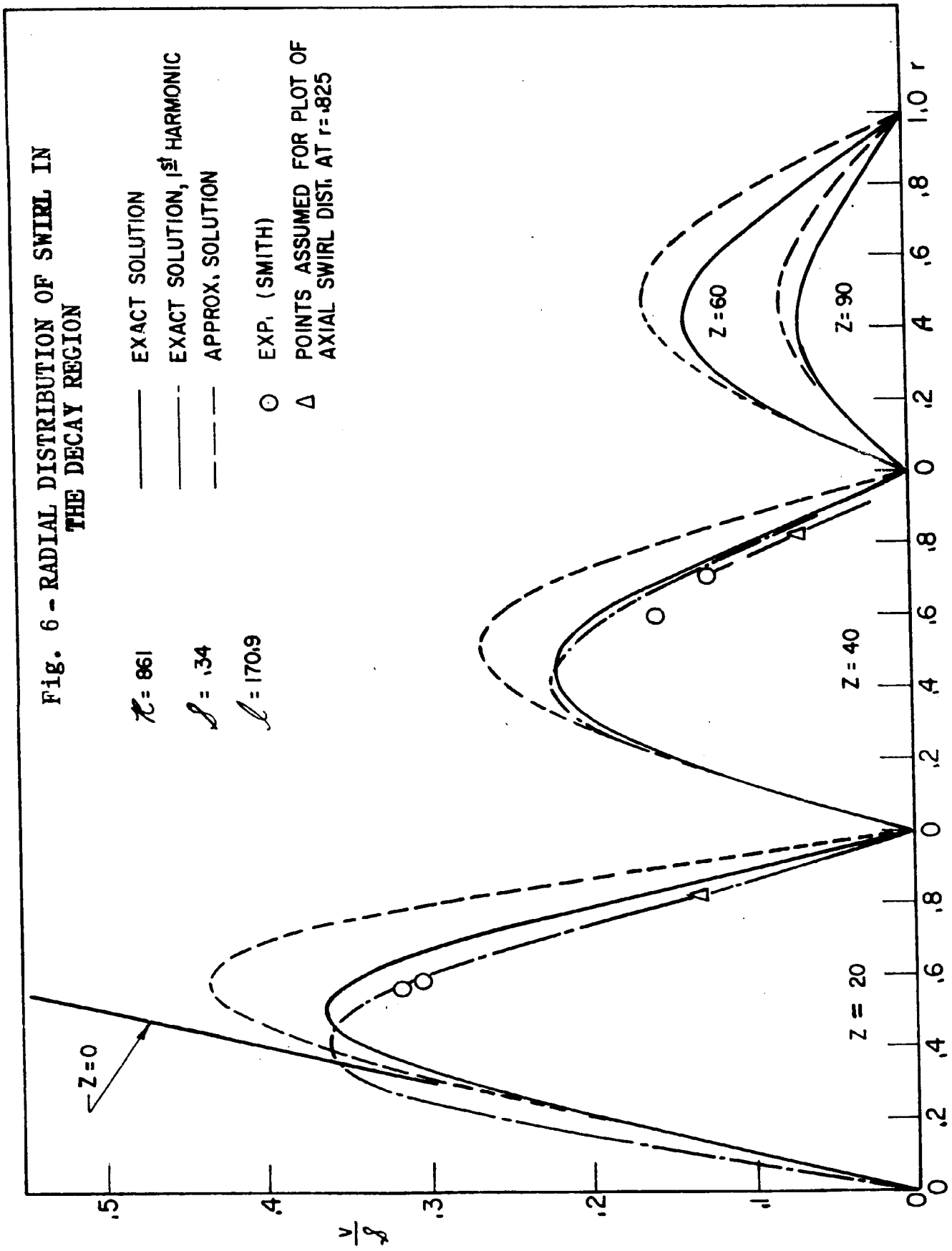


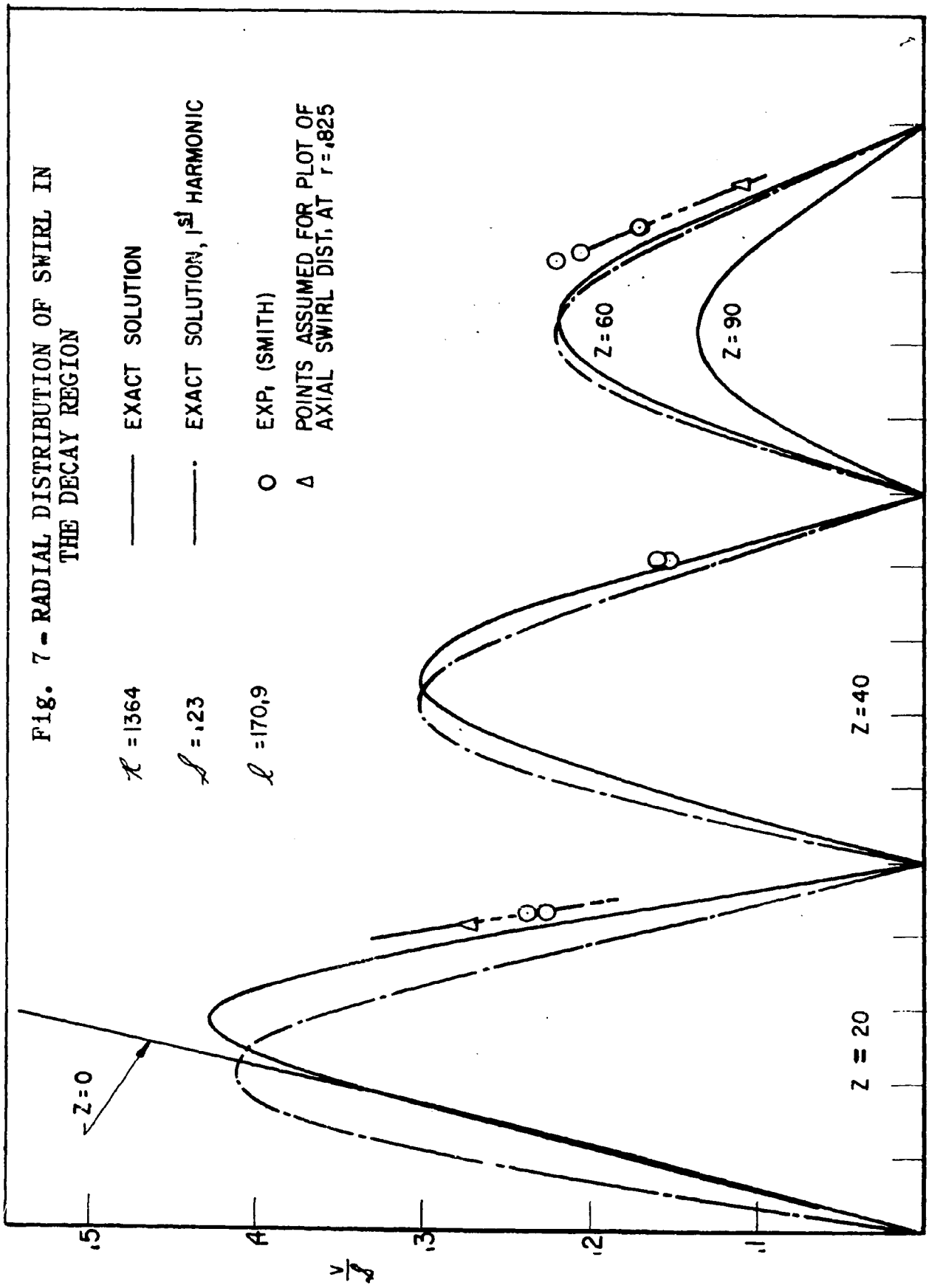
Fig. 2 - VALUES OF THE PARAMETERS AT THE INCEPTION OF SWIRL INSTABILITY IN THE DECAY REGION

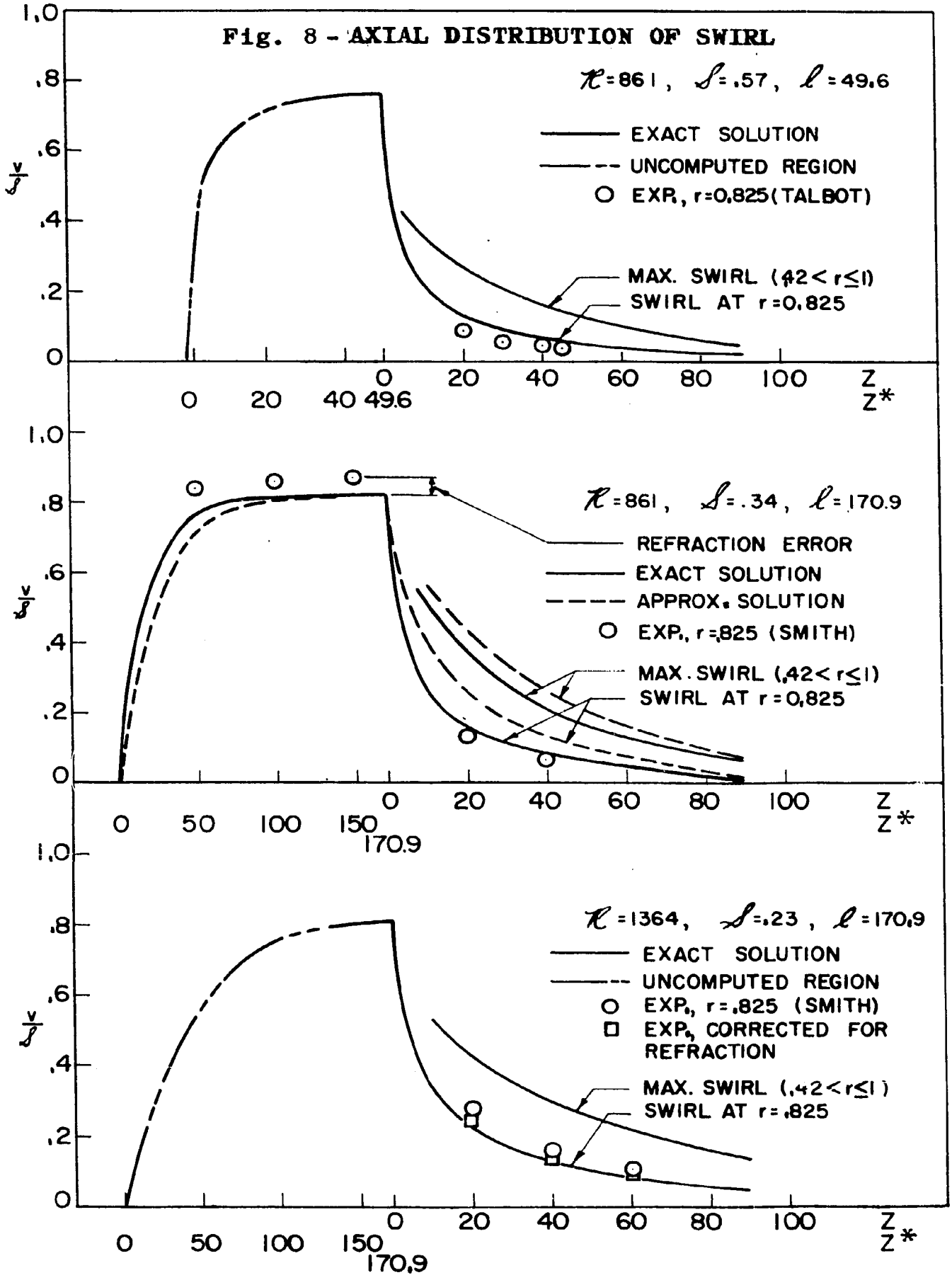

Fig. 3 - EIGENFUNCTIONS OF THE EXACT AND APPROXIMATE SWIRL SOLUTIONS
$J_1(\sqrt{\frac{2}{3}\mathcal{C}\beta_1}\,r)$
$R_1(r)$
$R_2(r)$
$R_3(r)$
$R_n(r)$
r
+1.0
+.8
+.6
+.4
+.2
0
-.2
-.4
-.6
-.8
-1.0
.2
.4
.6
.8
1.0
$R_n(r) = 2\lambda_n^{1/2} e^{-2\lambda_n r^2} \phi(1-\lambda_n; 2; 4\lambda_n r^2)$
Where
$16\lambda_n^2 \equiv \mathcal{C}\beta_n$

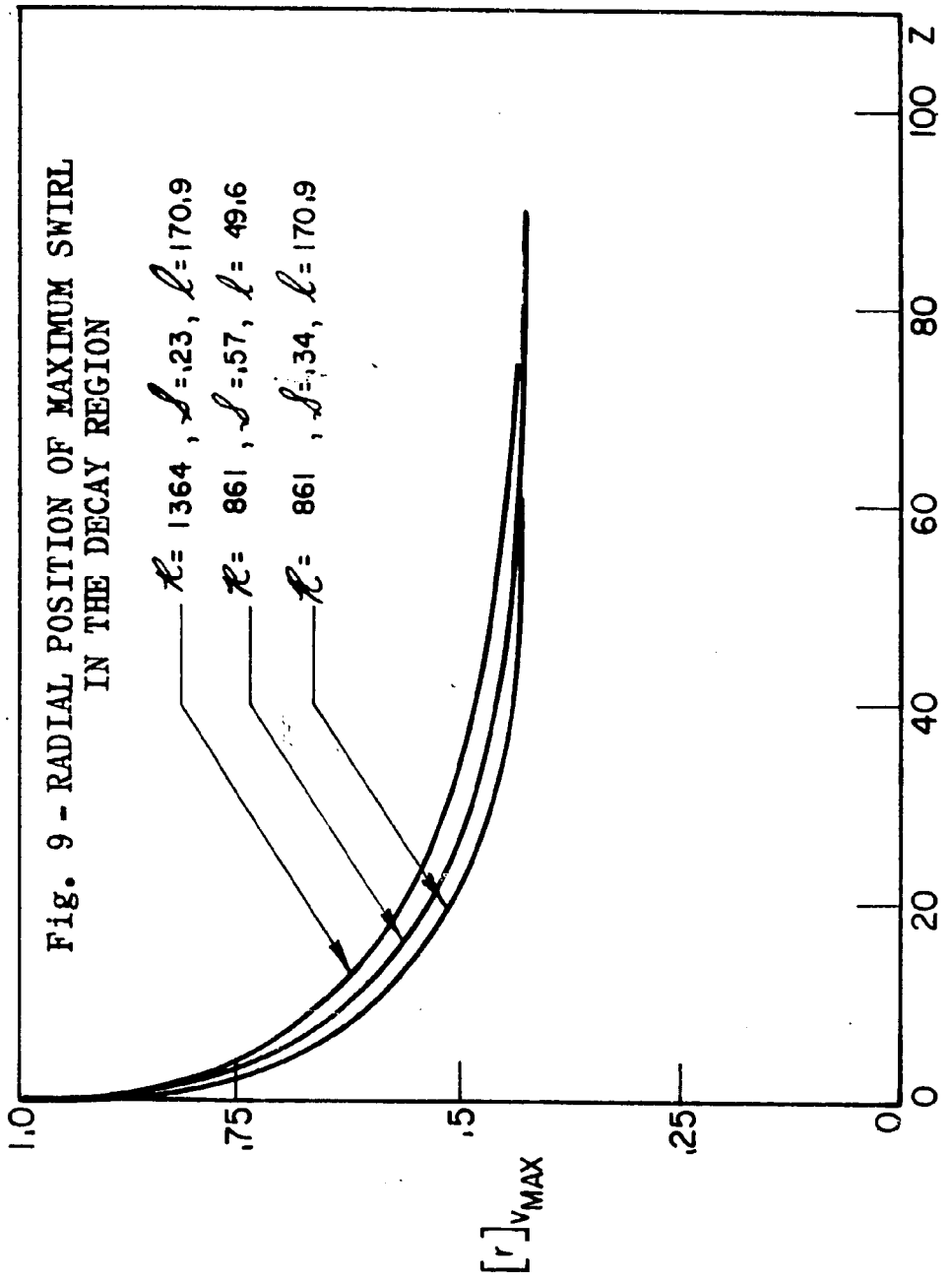

Fig. 4 - RADIAL DISTRIBUTION OF SWIRL IN THE DECAY REGION
κ = 861
δ = .57
ℓ = 49.6
EXACT SOLUTION
EXACT SOLUTION, 1st HARMONIC
O EXP. (TALBOT)
Z = 0
Z = 20
Z = 40
Z = 60
Z = 90
v/δ
r
0
.1
.2
.3
.4
.5
.6
.8
1.0


Fig. 5 - RADIAL DISTRIBUTION OF SWIRL IN THE GROWTH REGION
$\mathcal{R}$ = 861
δ = .34
ℓ = 170.9
EXACT. SOL.
APPROX. SOL.
EXP. (SMITH)
POINTS FOR PLOT OF AXIAL SWIRL DISTRIBUTION
APPROX. RE-FRACTION ERROR AT r = .825
z^* = 150, 170.9
z^* = 100
z^* = 50
$\frac{v}{\delta}$
r


Fig. 6 - RADIAL DISTRIBUTION OF SWIRL IN THE DECAY REGION
EXACT SOLUTION
EXACT SOLUTION, 1st HARMONIC
APPROX. SOLUTION
EXP. (SMITH)
POINTS ASSUMED FOR PLOT OF AXIAL SWIRL DIST. AT r=.825
R = 861
S = .34
L = 170.9
Z=0
Z = 20
Z = 40
Z=60
Z=90
v/S
r


Fig. 7 - RADIAL DISTRIBUTION OF SWIRL IN THE DECAY REGION
$\mathcal{K}$ = 1364
$\mathcal{S}$ = 1.23
$\mathcal{L}$ = 170.9
EXACT SOLUTION
EXACT SOLUTION, 1st HARMONIC
EXP, (SMITH)
POINTS ASSUMED FOR PLOT OF AXIAL SWIRL DIST. AT r = .825
Z = 0
Z = 20
Z = 40
Z = 60
Z = 90
v/s
r


Fig. 8 - AXIAL DISTRIBUTION OF SWIRL
$\mathcal{R}$=861, $\mathcal{S}$=.57, ℓ=49.6
EXACT SOLUTION
UNCOMPUTED REGION
EXP., r=0.825(TALBOT)
MAX. SWIRL (.42< r≤1)
SWIRL AT r=0.825
v/f
Z
Z*
$\mathcal{R}$=861, $\mathcal{S}$=.34, ℓ=170.9
REFRACTION ERROR
EXACT SOLUTION
APPROX. SOLUTION
EXP., r=.825 (SMITH)
MAX. SWIRL (.42< r≤1)
SWIRL AT r=0.825
$\mathcal{R}$=1364, $\mathcal{S}$=.23, ℓ=170.9
EXACT SOLUTION
UNCOMPUTED REGION
EXP., r=.825 (SMITH)
EXP., CORRECTED FOR REFRACTION
MAX. SWIRL (.42< r≤1)
SWIRL AT r=.825


Fig. 9 - RADIAL POSITION OF MAXIMUM SWIRL IN THE DECAY REGION
$\mathcal{K}$= 1364 , $\mathcal{S}$=.23, ℓ=170.9
$\mathcal{K}$= 861 , $\mathcal{S}$=.57, ℓ= 49.6
$\mathcal{K}$= 861 , $\mathcal{S}$=.34, ℓ=170.9
$[r]_{V_{MAX}}$
1.0
.75
.5
.25
0
0
20
40
60
80
100
Z

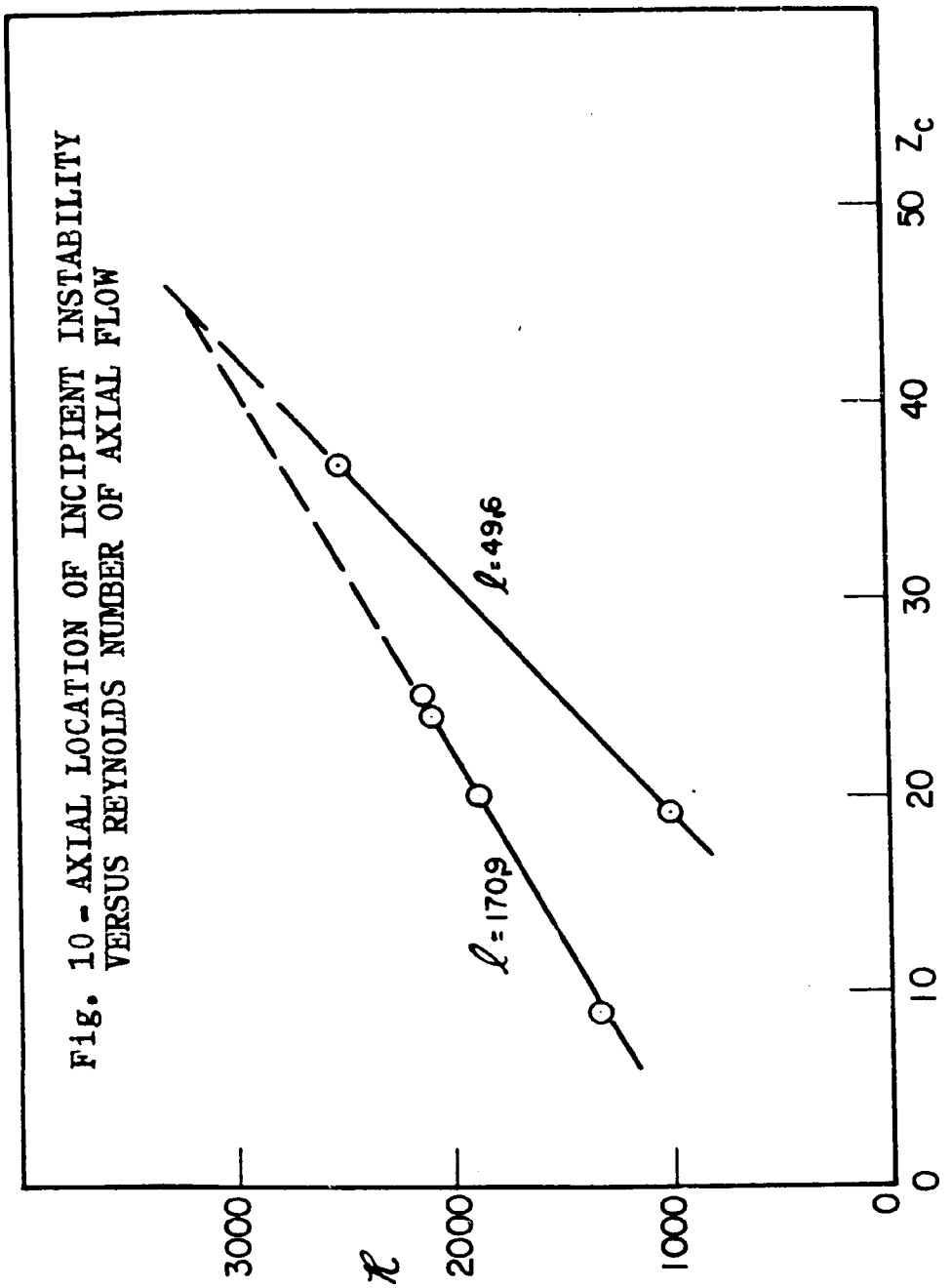


Fig. 10 - AXIAL LOCATION OF INCIPIENT INSTABILITY VERSUS REYNOLDS NUMBER OF AXIAL FLOW

Fig. 11 - TERMS AND PARTIAL SUMS OF THE EIGENFUNCTION EXPANSION OF $\bar{v}_o(r)$

